RESEARCH MEMORANDUM

WING-FLOW INVESTIGATION OF THE CHARACTERISTICS OF SEVEN UNSWEPT, UNTAPERED AIRFOILS OF ASPECT RATIO 8.0

By Harold L. Crane and James J. Adams

Langley Aeronautical Laboratory
Langley Field, Va.

NATIONAL ADVISORY COMMITTEE
FOR AERONAUTICS

WASHINGTON
June 13, 1951

NATIONAL ADVISORY COMMITTEE FOR AERONAUTICS

RESEARCH MEMORANDUM

WING-FLOW INVESTIGATION OF THE CHARACTERISTICS OF SEVEN UNSWEPT, UNTAPERED AIRFOILS OF ASPECT RATIO 8.0

By Harold L. Crane and James J. Adams

SUMMARY

A series of seven 10-percent-thick unswept and untapered airfoils of aspect ratio 8.0 have been tested by the wing-flow method at Mach numbers from 0.65 to 1.08 and a Reynolds number of approximately 700,000. The sections of the airfoils tested are as follows: (1) NACA 65-010, (2) NACA 65-210, (3) NACA 836D110, (4) NACA 847B110, (5) 10-percent-thick section with 3-to-1 elliptical nose and long straight-sided afterbody, (6) Thickness distribution of airfoil (5) and reflex mean line obtained from the difference between an NACA 420 and an NACA 240 camber line, and (7) Thickness distribution of airfoil (1) and camber line of airfoil (6).

The most significant feature of the results was the occurrence of an unstable pitching-moment variation with angle of attack for small angles of attack at Mach numbers of 0.85 to 0.90 for all the airfoils which had a conventional thickness distribution. This instability was not present for airfoils (5) and (6) which had blunt noses and straight-sided afterbodies with small trailing-edge angles. At the test Reynolds numbers the over-all aerodynamic characteristics of the blunt-nosed airfoils were undesirable, however, because of high drag and loss in lifting effectiveness at very small angles of attack. The use of the mean line obtained by subtracting an NACA 240 from an NACA 420 mean line, thereby confining the curvature to a small region near the nose, reduced the large changes in angle of zero lift such as were encountered by the NACA 65-210 airfoil through the transonic speed range. The pitching-moment characteristics were not improved, however, and an increase in drag resulted. In addition, it appears from these results that, for a reflex-cambered airfoil with the point of inflection near the leading edge, separation will be likely to occur at a small positive angle of attack due to the predominating influence of the negative camber on the rear portion of the airfoil. Subject to the low Reynolds numbers and other limitations of the wing-flow method, the NACA 65-010, 65-210, and 847B110 airfoils had more desirable over-all aerodynamic characteristics in the transonic speed range than the other airfoils tested.

INTRODUCTION

A series of investigations of the characteristics of airfoils and airfoil sections at transonic speeds are being conducted by the wing-flow method. In the present investigation the characteristics of seven 10-percent-thick airfoils all having the same plan form with 0° sweep, a simulated aspect ratio of 8.0, and a taper ratio of 1.0 were measured. The purpose of the investigation was to obtain data which would be useful in making selections of airfoils for transonic applications such as, for example, sweptback wings having camber and twist. The use of cambered airfoils or airfoils with large leading-edge radii would appear desirable to improve the maximum-lift characteristics and reduce the tip-stalling tendencies of such wings at low speeds. The present tests included airfoils with camber lines which were intended to reduce the undesirable effects of camber at transonic speeds. In addition, two blunt-nosed airfoils were included to determine the effects of this feature on the transonic characteristics. More complete information about the test airfoils is given in the section "DESCRIPTION OF TEST AIRFOIL SECTIONS."

Measurements were made of normal force, chord force, and pitching moment at angles of attack from approximately -6° to approximately 14°. The Mach number range was from 0.65 to 1.08 at Reynolds numbers between 650,000 and 750,000. Data were also obtained on one model of the series with a narrow strip of fine carborundum particles on either surface near the leading edge.

This paper presents and discusses the data obtained.

DESCRIPTION OF TEST AIRFOIL SECTIONS

The seven airfoils which have been tested were all 10 percent thick and are shown in figure 1. The figure shows both the design contour and a typical actual contour at one spanwise station for each airfoil. Two NACA 65-series airfoils, 65-010 and 65-210, were included because they were considered to be representative of common usage for airplanes designed to operate at the upper end of the subsonic speed range.

Two airfoils, NACA 836D110 and 847B110, of a series which was recently developed at the Ames Laboratory (reference 1) were included to determine whether the characteristics which were exhibited up to a Mach number $M = 0.85$ in the wind tunnel would be present throughout the transonic speed range. The NACA 8-series airfoils were developed with the object of eliminating the variation with Mach number of the angle of attack to maintain the design lift coefficient. The design principle

which was used is discussed thoroughly in reference 1, which also presents two-dimensional test results up to approximately M = 0.88 for the 8-series airfoils. Briefly, the 8-series airfoils were designed to induce by means of reflex camber a growth in the boundary layer on the lower surface to match the growth in boundary layer on the upper surface due to compressibility effects and thus to eliminate any change in the effective camber.

Two blunt-nosed airfoils were also included. The first was an uncambered airfoil with a 3-to-1 elliptical nose which faired into a long straight-sided afterbody. According to a correlation of maximum-lift data by Multhopp in reference 2 this airfoil should have approximately the optimum bluntness for developing maximum lift coefficient and therefore should develop as much as 0.3 higher lift coefficient than the NACA 65-series airfoils. It was thought that the long straight-sided afterbody would minimize changes in moment characteristics in the transonic speed range.

The other blunt-nosed airfoil had the same thickness distribution but was cambered for a design lift coefficient of 0.3 using a mean line determined by subtraction of an NACA 240 from an NACA 420 camber line. This combination of mean lines results in an S-shaped camber line such as is the case with airfoils of the 8-series, but which has the point of inflection farther forward. It was thought that a camber line which confined the lack of symmetry to a small region near the leading edge might reduce pitching-moment variations and/or changes in the angle of zero lift in the transonic range. The seventh test airfoil combined the thickness distribution of the NACA 65-010 airfoil with the camber line obtained from the difference of the NACA 420 and 240 mean lines. It should be noted from figure 1 that the fabrication of this airfoil was poor with the result that the nose of the airfoil was sharp-edged.

APPARATUS AND PROCEDURE

Figure 2 gives details and dimensions of the plan form and installation used in these tests. The models were made of 75S-T aluminum alloy. The chord of each model was 2 inches and the semispan 8 inches. A circular end plate 1/32 inch thick was used to act in conjuction with the test panel as a reflection plane to simulate full-span conditions. The gap between the end plate and the test panel was approximately 0.1 inch.

For one flight the leading edge of the NACA 65-010 airfoil was roughened on both surfaces with a strip of 0.002-inch carborundum particles imbedded in shellac. The roughness strips were approximately 0.1 inch wide and were located 0.05 inch back from the leading edge.

The models were mounted on the right wing of a fighter-type airplane. A close-up of one of the airfoils mounted on the test panel is shown in figure 3. The flow-direction vane is also visible in the photograph. The contour of a portion of the wing had been modified to reduce the velocity gradient across the model and to place the wing compression shock behind the model.

Plots of the chordwise and vertical Mach number gradients in the test region are presented in figure 4. A chart was prepared, from the pressure-distribution data for the test panel, of the average Mach number of the flow over the model as a function of airplane Mach number and lift coefficient. In the reduction of data this chart was used to determine the Mach number at the model, which, in turn, was used to determine the dynamic pressure at the model.

The aerodynamic forces and moments were measured with a deflection type of balance which was equipped with autosyn pickups. The attitude angle and the angle of flow were also recorded through autosyn pickups and the five variables, normal force, chord force, pitching moment, attitude angle, and the angle of flow, were recorded continuously on a single film.

Since the flow direction vane was mounted 22 inches outboard of the model, it was necessary to apply a correction for the difference in angle of flow between the vane location and the model location. The angle of attack was the sum of the attitude angle and the corrected angle of flow. Airspeed, altitude, normal acceleration, and free-air temperature were recorded with standard NACA instruments.

During flight the attitude angle of the test model was varied continuously from -6° to 14° at approximately 1 cycle per second by an electric actuator. This rate of oscillation resulted in a maximum rate of pitching of the order of 1° per 80 chords of motion with respect to the air stream, which is believed to be sufficiently small to approximate static conditions.

The data were obtained in a dive and pull-out which was designed to yield the maximum Reynolds number obtainable at any Mach number within the limits of safe operation of the airplane. The test runs were recorded starting at an airplane Mach number of 0.73 at 15,000 feet and holding an indicated airspeed of 450 miles an hour with a pull-out to level flight at 5,000 feet. With this procedure the test Reynolds number remained between 650,000 and 750,000.

PRESENTATION OF RESULTS

An example of the wing-flow data showing the test points is presented in figure 5. In subsequent figures no test points are shown in order that it be possible to present data for Mach numbers throughout the test range on a single figure. An indication of the accuracy of the various measurements is presented in the following table:

Variable	Estimated possible error in -	
	Absolute value	Coefficient
Mach number, M	±0.01	
Dynamic pressure, q, percent	±2.0	
Angle of attack, α, degrees	±0.5	
Normal force, N, pounds	±2.0	±0.04
Chord force, C, pounds	±0.25	±0.005
Pitching moment, M, inch-pounds	±1.0	±0.01

The errors in coefficients are presented for the minimum dynamic pressure, which was 80 inches of water. These errors would tend to be reduced slightly at the maximum dynamic pressure of 150 inches. It should be noted that because of the nature of the instrumentation, errors in increments of any measured variable determined from the faired curves presented herein will be smaller than errors in absolute values. The values of chord force and drag have not been corrected for the drag of the end plate or model shank or for any interference effects. Previous attempts to measure the drag of the end plate in the presence of the model have not been successful.

Figures 6 to 12 present summary plots at Mach numbers throughout the test range of the variations of normal-force, chord-force, and pitching-moment coefficients with angle of attack for each of the seven airfoils tested. The increments of Mach number in the presentation are usually 0.05 but in some cases near $M = 0.85$ where large changes in characteristics occur, the Mach number increments are reduced to 0.025. At somewhat larger Mach number intervals, the data have been converted to lift and drag coefficients and are plotted in polar form in figure 13. Figures 14 to 20 are for the most part cross plots of the data obtained, which were prepared to aid in the analysis of the data. Figure 16 is a comparison of the results obtained on the NACA 65-010 airfoil with and without leading-edge roughness.

DISCUSSION OF RESULTS

The results of the wing-flow tests of this series of airfoils are discussed largely from the standpoint of what effect the airfoil characteristics would have on the longitudinal stability of a complete airplane configuration. The longitudinal stability of a complete configuration depends upon the downwash field produced by the wing as well as on the lift and pitching-moment characteristics of the wing. Since no measurements of downwash were obtained and since in any case the effects of the airfoil characteristics on the longitudinal stability of a complete airplane configuration depend upon the geometry of the configuration, the discussion must be regarded as qualitative. Nevertheless, airfoils which experience smaller changes in lift and moment characteristics in the transonic range may be considered to be more favorable from the standpoint of longitudinal stability and trim changes.

It should be noted that the detailed cross plots of the data which are presented were included only in an attempt to establish the relative merits of the various airfoils at transonic speeds. Because of the low Reynolds numbers and other limitations of the test method, these figures should not be considered valid as design charts for full-scale configurations.

Lift Characteristics

Changes in the angle of zero lift or in lift-curve slope with Mach number are likely to result in undesirable trim changes. The relative magnitude of the variation of the angle of zero lift with Mach number for the test airfoils is illustrated by figure 14, which also presents the variation of angle of attack with Mach number required to maintain constant lift coefficients of 0.1, 0.2, and 0.3. In this respect the characteristics of the blunt-nosed airfoils were more favorable than the single-cambered NACA 6- and 8-series airfoils. The variation of angle of attack for constant lift coefficient was considerably larger for the NACA 65-210 airfoil than for any other of the airfoils tested. At transonic speeds the reflex-cambered airfoil, having approximately the thickness distribution of the NACA 65-210 airfoil, had a much smaller variation of angle of attack with Mach number for constant, small values of lift coefficient than the NACA 65-210 airfoil. At subsonic speeds and small angles of attack the effective camber of the two airfoils was approximately equal. However, the reflex-cambered airfoil was subject to separation at a smaller angle of attack. Susceptibility of this airfoil to separation was probably aggravated by the inadvertently sharpened leading edge.

[redacted]

The variation with Mach number of the slope of the normal-force curves at angles of attack of 0° and 4° (which, at small angles of attack, very closely approximate the lift curves) are presented in figure 15 for the seven test airfoils. The over-all tendency was toward a moderate decrease in C_{N_α} with increasing Mach number over the test range. Reexamination of figures 6 to 12 shows that below the stall the lift curves of all test airfoils were more nonlinear at Mach numbers of 0.80 to 0.90 than elsewhere in the speed range. In most cases, as shown in figure 15(a), the slope C_{N_α} at small angles of attack was at a minimum in this Mach number range. For the uncambered airfoil with the elliptical nose, however, C_{N_α} for $\alpha = 0°$ passed through the maximum at a Mach number of 0.85. In general the NACA 6- and 8-series airfoils and the cambered elliptical-nosed airfoil had a less erratic and therefore probably more acceptable variation of lift-curve slope with Mach number than the uncambered elliptical-nosed airfoil.

The airfoils all showed a loss in lifting effectiveness at low angles of attack at the lower test Mach numbers, such as was the case for the NACA 65-010 airfoil at an angle of attack of 8° and a Mach number of 0.65. (See fig. 6.) Corresponding changes in the slope of the chord-force and moment curves which occurred at the same angles of attack are indicative of flow separation. This flow condition would very likely occur at higher angles of attack at higher Reynolds numbers.

The earliest reduction in lifting effectiveness occurred with the blunt-nosed airfoils. The data of figure 10 indicate that the uncambered elliptical-nosed airfoil was subject to loss in lifting effectiveness at approximately 4° at a Mach number of 0.65. The reflex-cambered elliptical-nosed airfoil underwent a reduction in lifting effectiveness at 2°. (See fig. 11.) However, at negative angles the loss in lifting effectiveness did not occur until an angle of attack of 6°, which would indicate that the inverted NACA 240 camber line seems to predominate. Application of the reflex-camber line to an airfoil having the NACA 65-010 thickness distribution except for the inadvertently sharpened nose also resulted in an earlier break in the lift and pitching-moment curves. (See fig. 12.) In this case, however, it is uncertain whether the camber or the sharpened nose was primarily responsible.

According to a correlation of maximum-lift data by Multhopp (reference 2) the blunt-nosed airfoils tested should have a high maximum lift coefficient. However, tests in the Langley two-dimentional low-turbulence tunnel (reference 3) have indicated that a Reynolds number of several million would be required to realize the maximum attainable lift coefficient.

A second test run was made with the NACA 65-010 airfoil model with leading-edge roughness strips installed on both surfaces. The strips were approximately 0.1 inch wide, were located 0.05 inch back from the leading edge, and consisted of fine carborundum particles 0.002 inch in diameter fastened in place with shellac. Data for the NACA 65-010 airfoil with and without leading-edge roughness are presented in figure 16 for three Mach numbers. The roughness strips generally decreased the rate of change of normal-force coefficient with angle of attack at the lower test Mach numbers and decreased the abruptness of the loss in lifting effectiveness at the stall. At the higher test Mach numbers the force and moment characteristics were very little affected by leading-edge roughness.

Moment Characteristics

The principal point of interest immediately apparent from these data is the type of moment variation encountered near a Mach number of 0.85. It is apparent from figures 6 to 12 that the NACA 6- and 8-series airfoils had an S-shaped variation of pitching moment with angle of attack at Mach numbers in the region of 0.85 to 0.90 which resulted in an unstable slope at small angles of attack. This instability at small angles of attack amounted to a considerable aerodynamic-center shift, the magnitude of which is illustrated by figure 17, a plot of the variation of aerodynamic-center position with Mach number at $\alpha = 0^\circ$ and $\alpha = 4^\circ$ for all the test airfoils. Figure 17 shows that there was a general tendency for the aerodynamic center to move rearward gradually from approximately the quarter-chord point to the vicinity of the four-tenths-chord point as the Mach number increased from 0.65 to 1.08. This tendency was interrupted in the case of the NACA 6- and 8-series airfoils for $\alpha = 0^\circ$ at a Mach number of approximately 0.85 by a very marked forward movement of the aerodynamic center, a half chord ahead of the leading edge for the NACA 836D110 airfoil. Such a movement of the aerodynamic-center position would be highly objectionable if it occurred at full-scale Reynolds number with either an all-wing or a conventional airplane configuration, because it would result in longitudinal instability and possibly in a tendency to wing divergence. The NACA 847B110 airfoil had the smallest forward aerodynamic-center shift of the NACA 6- or 8-series airfoils, about 20 percent chord, and the uncambered, blunt, elliptical-nosed airfoil did not exhibit any appreciable shift.

The wind-tunnel data of reference 1 for the NACA 65-010, 836D110, and 847B110 airfoils, which were obtained at a Reynolds number of 1,900,000, did not show any evidence of instability at small angles of attack at $M = 0.85$ to 0.90. However, such an effect could have been camouflaged by the fact that $M = 0.85$ was close to the tunnel choking Mach number. Such instability has been noted during tests of several

NACA 6-series airfoils in the Langley 4- by 19-inch wind tunnel at transonic speeds and a Reynolds number of 1,400,000. Results of the 4- by 19-inch tunnel investigation have not yet been published. As yet, no verification of this effect at or near full-scale Reynolds numbers has been obtained, because of the limitations of existing testing facilities. At larger angles of attack the data of reference 1 show a much more rapid increase in the stability of the moment curves with increasing Mach number than does the wing-flow data. It is not certain whether this discrepancy is due to the lower Reynolds number of the wing-flow tests, to inadequacy of the technique of correcting the wind-tunnel moment data for wall interference effects, or to the fact that wing-flow models had a finite aspect ratio while the wind-tunnel models were two dimensional.

The variation with Mach number of pitching-moment coefficient for the seven test airfoils at a constant lift coefficients of 0.2 is presented in figure 18. These data show that all the test airfoils were subject to large and abrupt trim changes in the transonic region. In this respect the characteristics of the elliptical-nosed airfoils were perhaps the least objectionable.

The possibility is suggested that a reflex-cambered airfoil having a moderately blunt nose, which would correspond to a position of maximum thickness behind that of the elliptical-nosed airfoils tested (15 percent chord) but ahead of the positions of maximum thickness of the NACA 6- and 8-series airfoils tested (40 or 50 percent chord) could be developed to minimize trim changes in the transonic region.

Drag Characteristics

As has been stated in the presentation of results, the values of drag given in this paper include the drag of the end plate and any interference drag. However, the end-plate effects would be very nearly the same for all models. The drag characteristics of the test airfoils are illustrated in polar form in figure 13. It should be noted that the drag scale was varied to show the data more clearly. These data indicate that the drag of the elliptical-nosed airfoils was appreciably higher than that of the other test airfoils, but that within the accuracy of the data the NACA 6- and 8-series airfoils had approximately the same amount of drag.

The variation with Mach number of the maximum lift-to-drag ratios are presented in figure 19. Here again it is indicated that the NACA 6- and 8-series airfoils, except for the reflex-cambered airfoil with the NACA 65-010 thickness distribution, had the more favorable drag characteristics.

[redacted]

Figure 20, which is a plot of minimum drag coefficient against Mach number for the seven airfoils tested, shows that the minimum drag of the blunt, elliptical-nosed airfoils was noticeably higher, ΔC_D = 0.01 to 0.02, than the drag of the NACA 6- and 8-series models at Mach numbers of 0.65 to 1.10. It is likely that the minimum test Mach number (0.65), was above the critical Mach number for the elliptical-nosed airfoils. The drag rise occurred at a Mach number about 0.1 lower than was the case for the other test airfoils. Of the NACA 6- and 8-series airfoils, the NACA 65-010 airfoil had the lowest and the reflex-cambered airfoil with the approximate NACA 65-010 thickness distribution and the sharpened nose had the highest minimum drag coefficient. The differences between the minimum drag of the NACA 65-210, 836D110, and 847B110 airfoils were small enough to be within the accuracy of the data over most of the Mach number range. The drag rise due to increasing Mach number was approximately similar for each of the airfoils tested.

Figure 16 shows that the effect of leading-edge roughness on the NACA 65-010 airfoil was to increase the chord force somewhat but also to delay the effects of separation as the angle of attack increased.

It is interesting to note that according to the variation of chord force with angle of attack in figure 11, as well as the other data for the airfoil with elliptical nose and reflex camber, the negative angle of attack at which separation occurred at the lower test Mach numbers was approximately 8° compared to a value of approximately 2°, positive. It appears from these results that, for a reflex-cambered airfoil with the point of inflection near the leading edge, separation will be likely to occur at small positive angles of attack due to the predominating influence of the negative camber on the rear portion of the airfoil.

CONCLUDING REMARKS

The most significant feature of the results was the occurrence of unstable pitching-moment variations at small angles of attack at Mach numbers of 0.85 to 0.90 for all of the test airfoils except the two with blunt noses and small trailing-edge angles. This behavior would be very undesirable if it occurred at full-scale Reynolds numbers, because it would result in longitudinal instability and possibly in a tendency to wing divergence. Two-dimensional wind-tunnel tests of three of the airfoils at a Reynolds number of 1,900,000 did not exhibit this characteristic. Such a characteristic might have been camouflaged, however, by choking of the wind tunnel. Similar instability has been noted in transonic wind-tunnel tests at a Reynolds number of 1,400,000.

[redacted]

No verification of the effect at or near full-scale Reynolds numbers has been obtained, however. Tests to investigate this effect at higher Reynolds numbers would therefore be very desirable.

Although the moment characteristics of the blunt-nosed airfoils were desirable, at the test Reynolds numbers the over-all aerodynamic characteristics of the blunt-nosed airfoils were undesirable because of high drag and loss in lifting effectiveness at very small angles of attack. The airfoils which had the smallest forward aerodynamic-center shift with favorable characteristics in other respects were the NACA 847B110 and 65-210 airfoils.

It appears from these data that the camber obtained by subtracting an NACA 240 from an NACA 420 mean line when applied to the thickness distribution of the NACA 65-210 airfoil did result in a smaller variation of angle of attack for constant lift coefficient with Mach number but did not reduce the pitching tendencies. In addition, it appears from these results that, for a reflex-cambered airfoil with the point of inflection near the leading edge, separation will be likely to occur at a small positive angle of attack due to the predominating influence of the negative camber on the rear portion of the airfoil.

In most respects the characteristics of the NACA 6-series and 8-series airfoils were equally favorable. It is not felt, however, that the present investigation was sufficiently comprehensive because of low Reynolds numbers and other limitations to select any one of the 6- or 8-series airfoils tested as having the most desirable characteristics in the transonic speed range. The NACA 65-010, 65-210, and 847B110 airfoils had better over-all aerodynamic characteristics at transonic speeds than the other airfoils tested.

The possibility is suggested by the analysis of the results of this investigation that a reflex-cambered airfoil having a moderately blunt nose could be developed to minimize trim changes in the transonic region.

Langley Aeronautical Laboratory
National Advisory Committee for Aeronautics
Langley Field, Va.

REFERENCES

1. Graham, Donald J.: The Development of Cambered Airfoil Sections Having Favorable Lift Characteristics at Supercritical Mach Numbers. NACA Rep. 947, 1949.

2. Multhopp, H.: On the Maximum Lift Coefficient of Aerofoil Sections. TN No. Aero. 1980, British R.A.E., Dec. 1948.

3. Loftin, Laurence K., Jr., and Smith, Hamilton A.: Aerodynamic Characteristics of 15 NACA Airfoil Sections at Seven Reynolds Numbers from 0.7×10^6 to 9.0×10^6. NACA TN 1945, 1949.

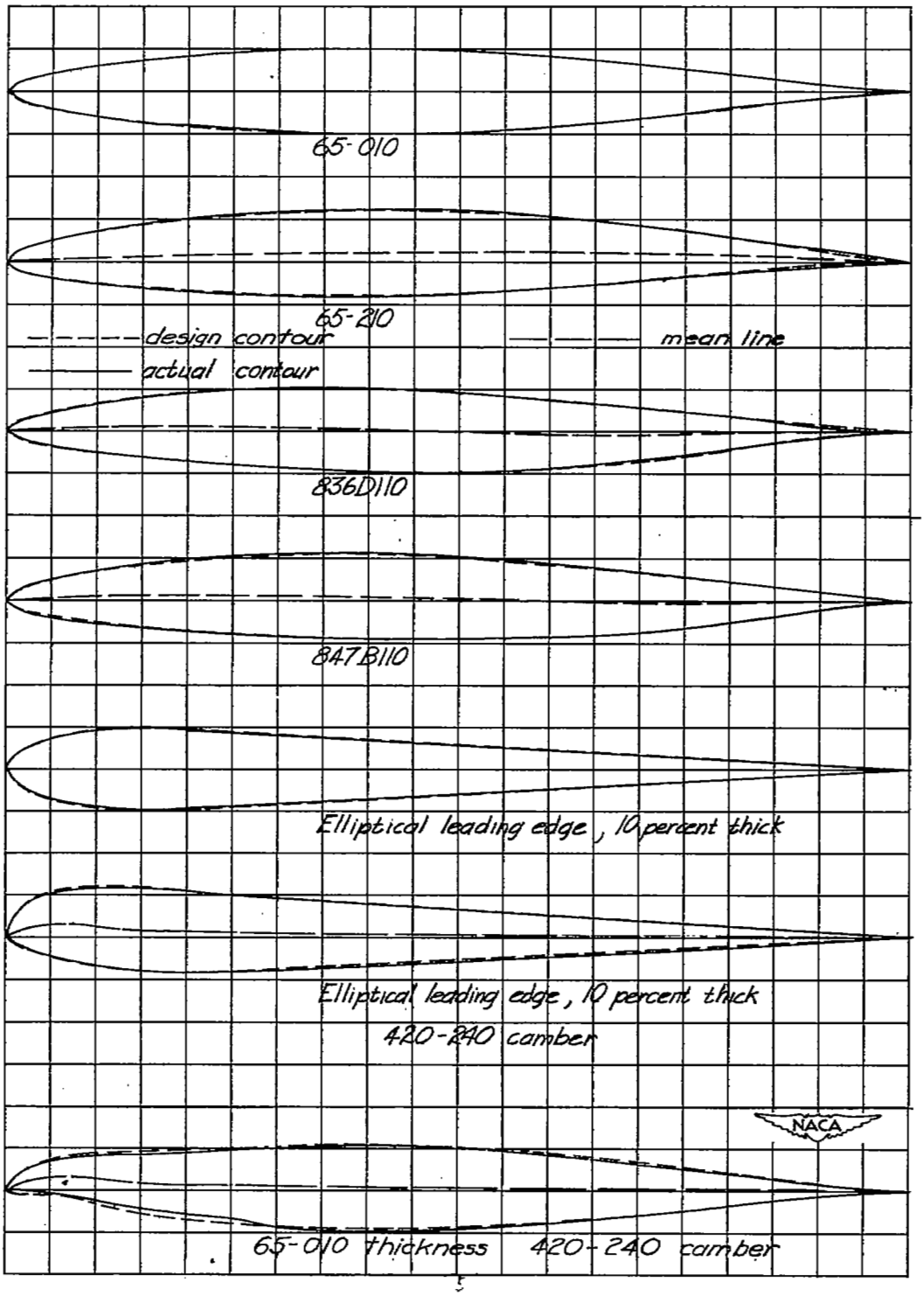

Figure 1.- Design contour and actual contour at one station of the test airfoils.

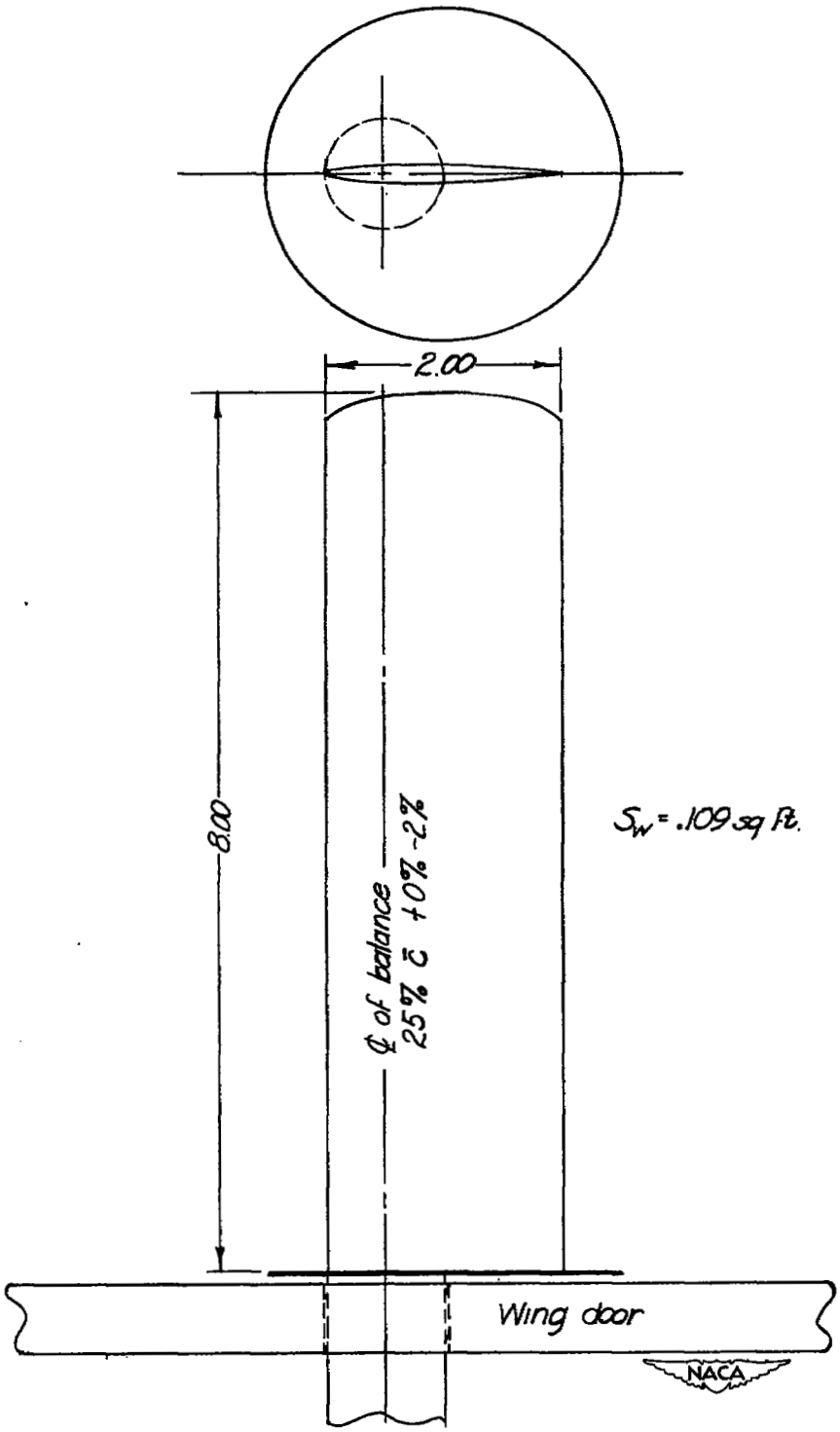

Figure 2.- Plan view, and view from the tip, of the airfoil installation.

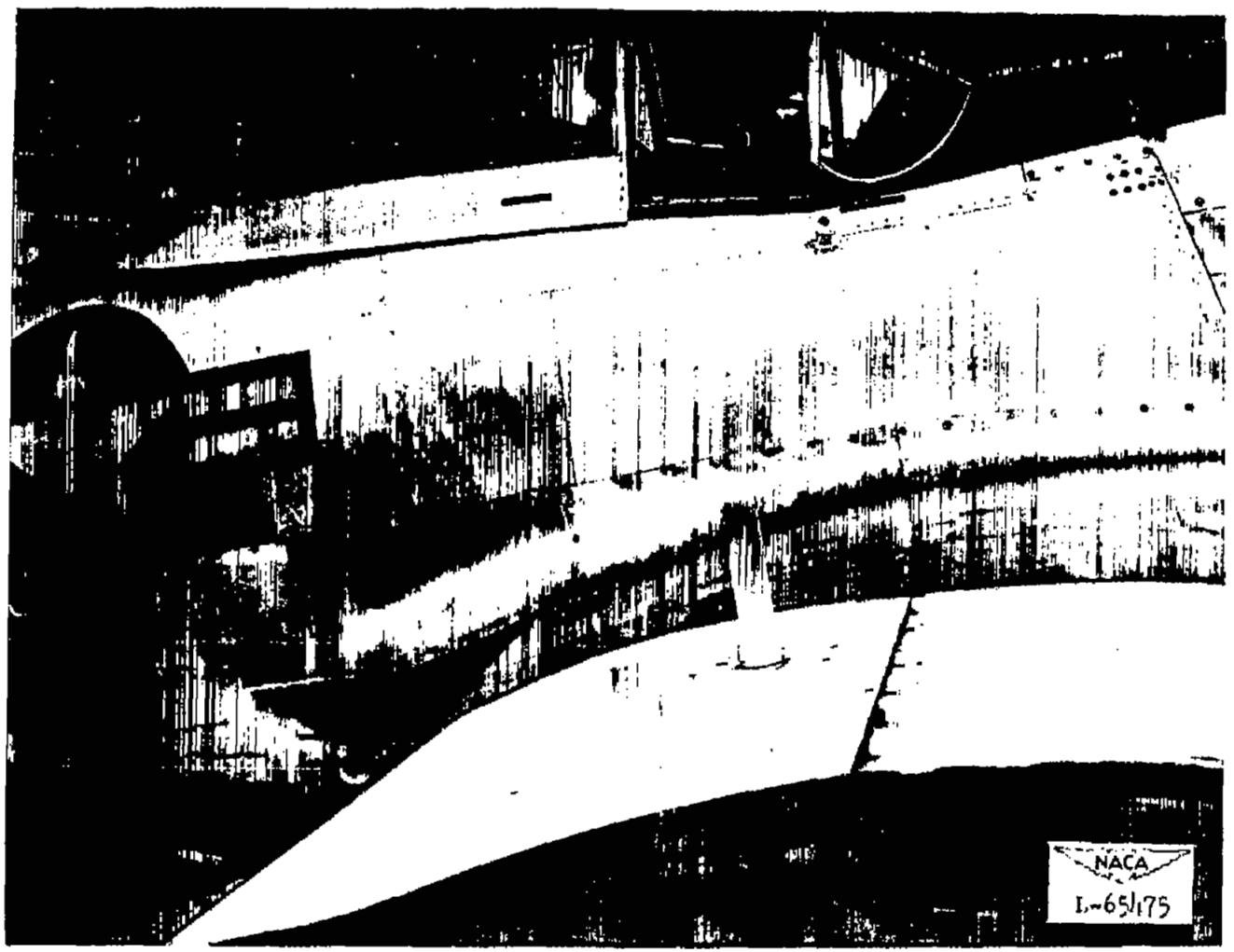

Figure 3.- Photograph of airfoil and flow-direction vane in place on wing-flow airplane.

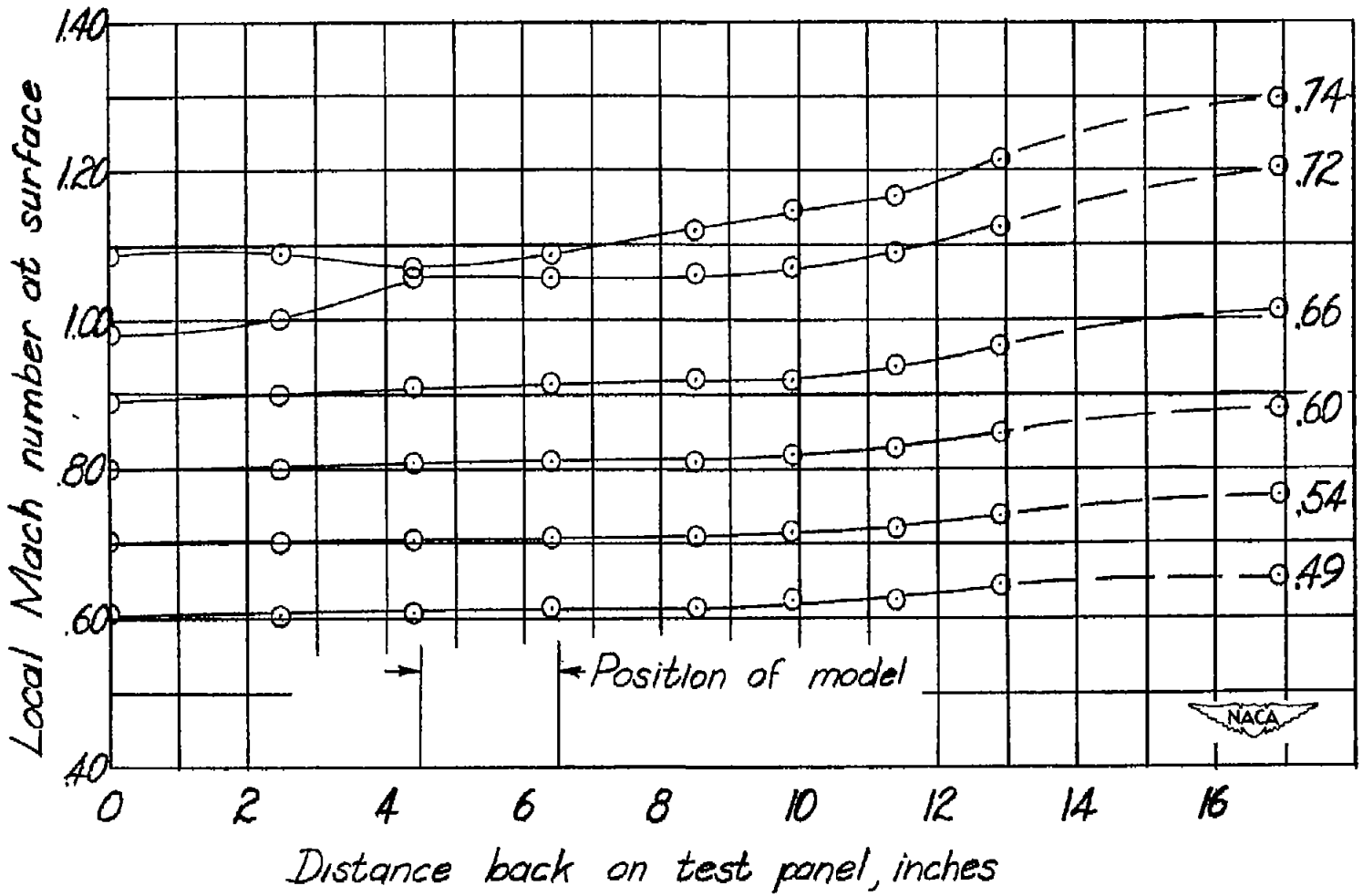

(a) Chordwise variation.

Figure 4.- Typical velocity gradients at test location.

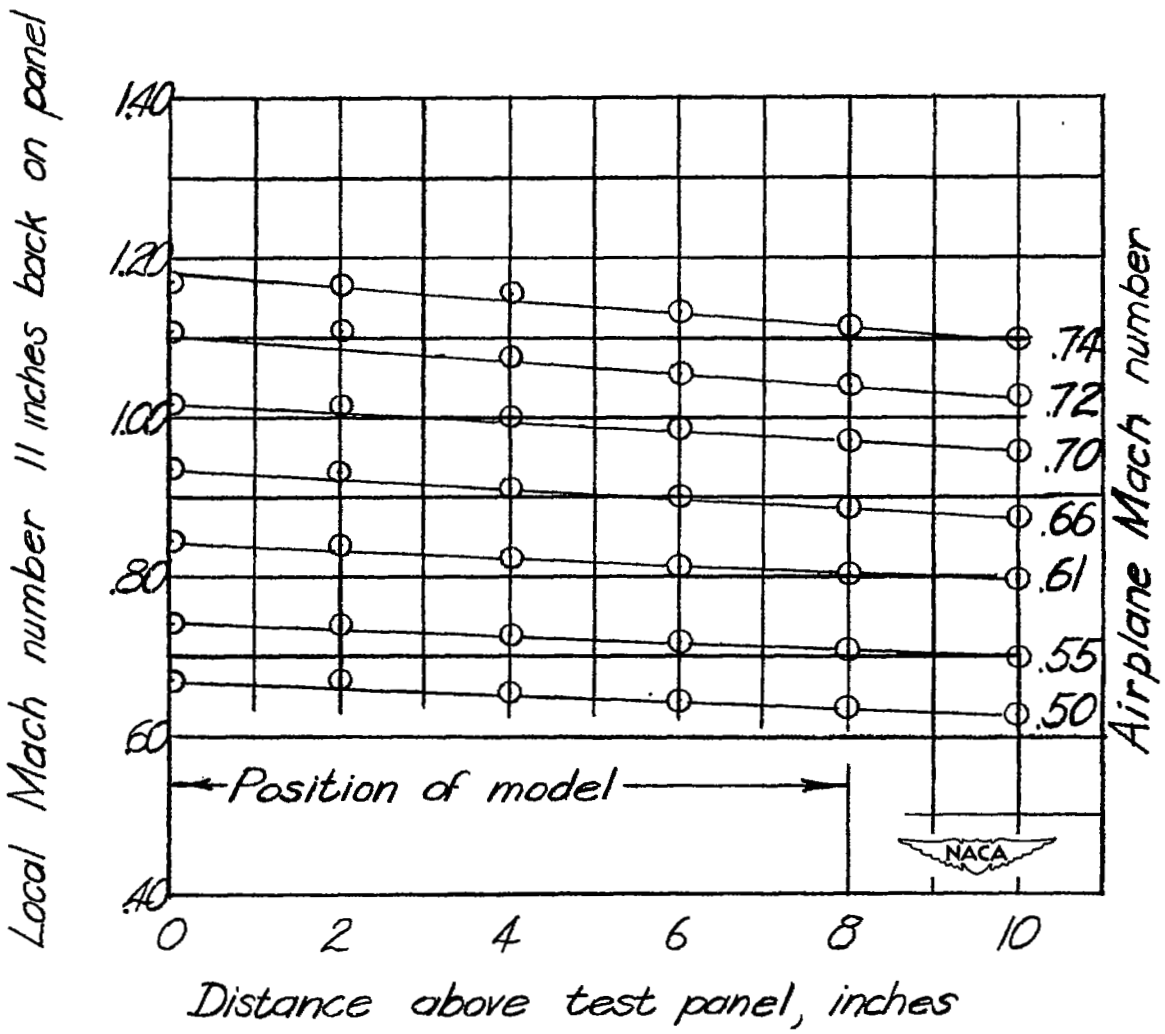

(b) Spanwise of the model.

Figure 4.- Concluded.

[redacted]

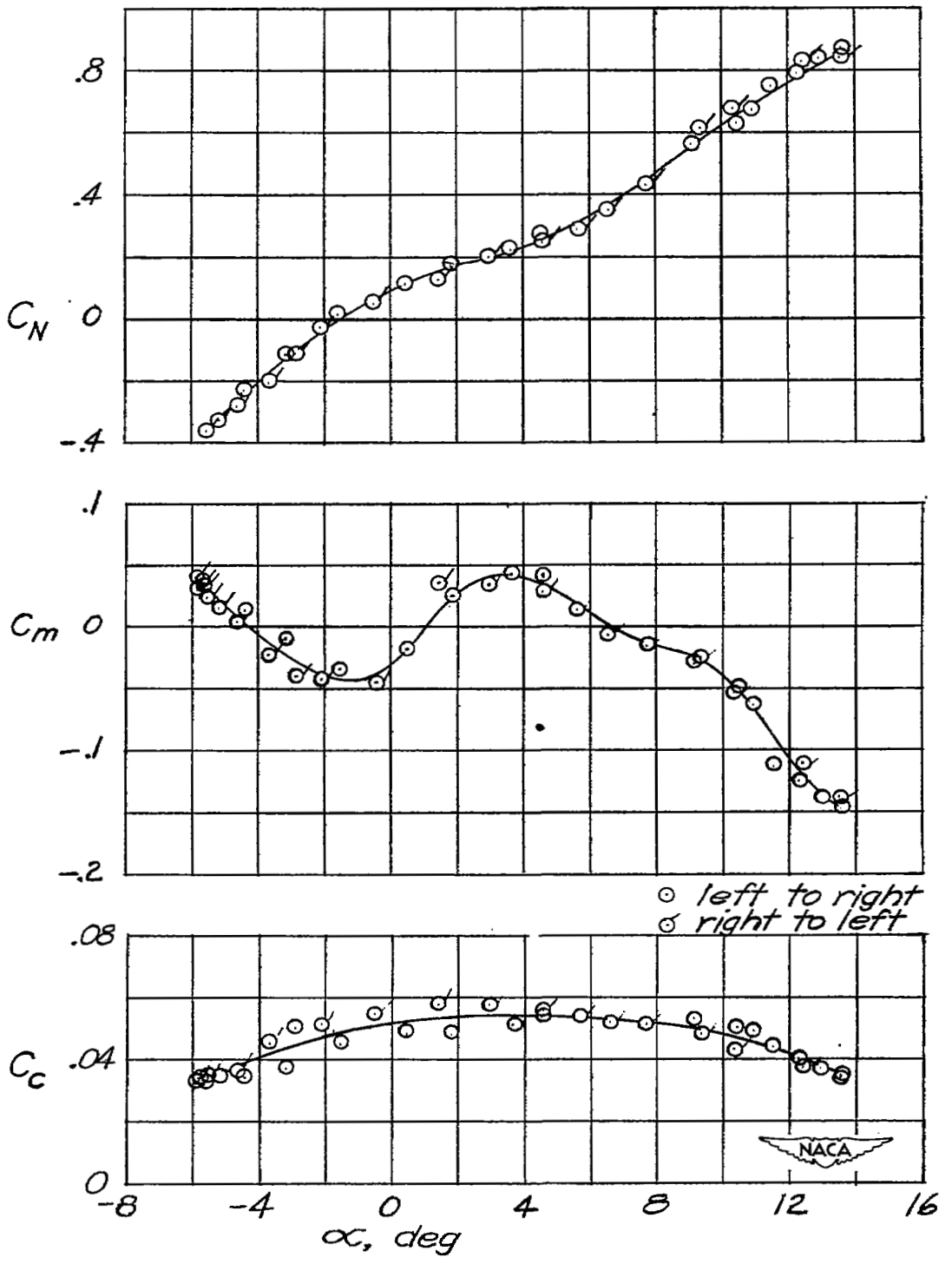

Figure 5.- Plot of test data as first obtained showing average amount of scatter. NACA 836D110 airfoil at M = 0.875.

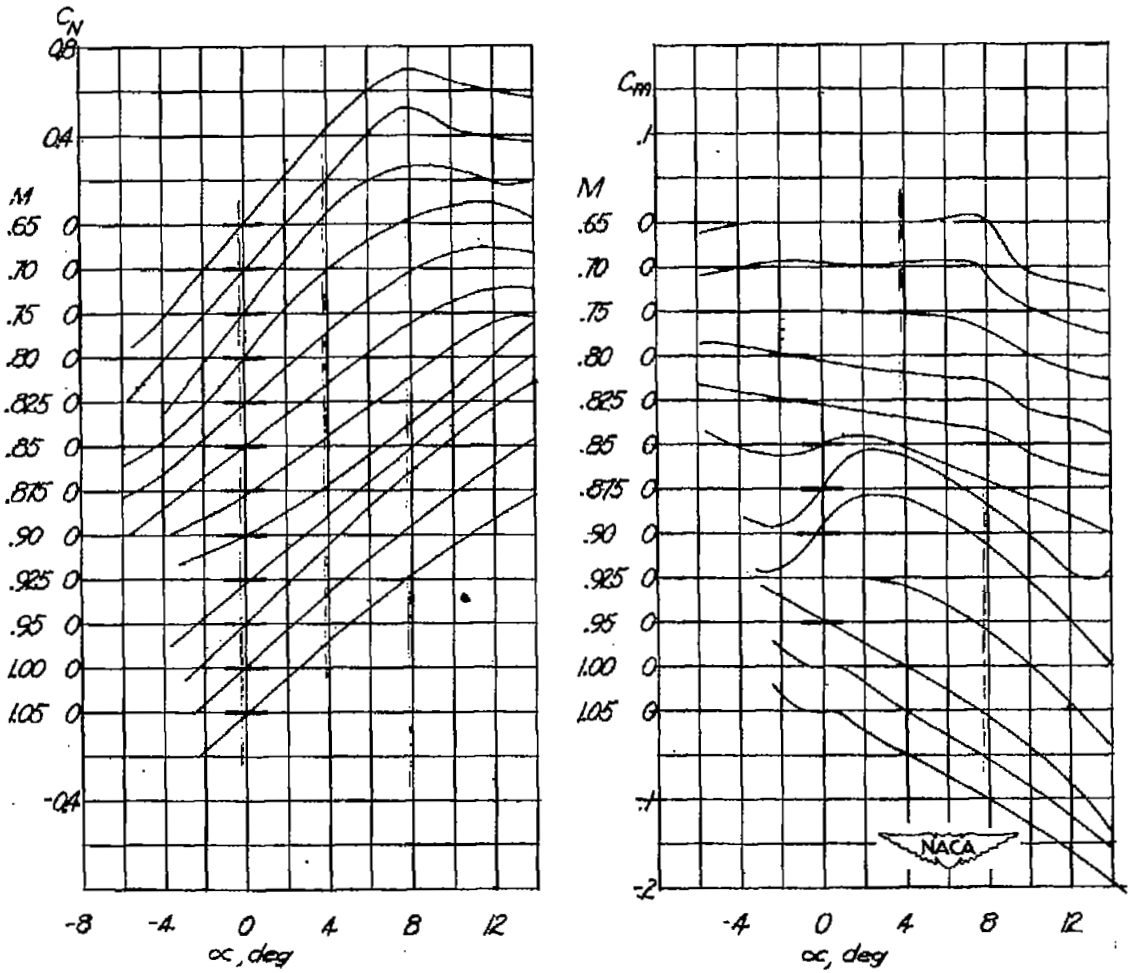

(a) Variation of normal-force and pitching-moment coefficients with angle of attack.

Figure 6.- Measured force and moment characteristics of NACA 65-010 airfoil at Mach numbers from 0.65 to 1.08.

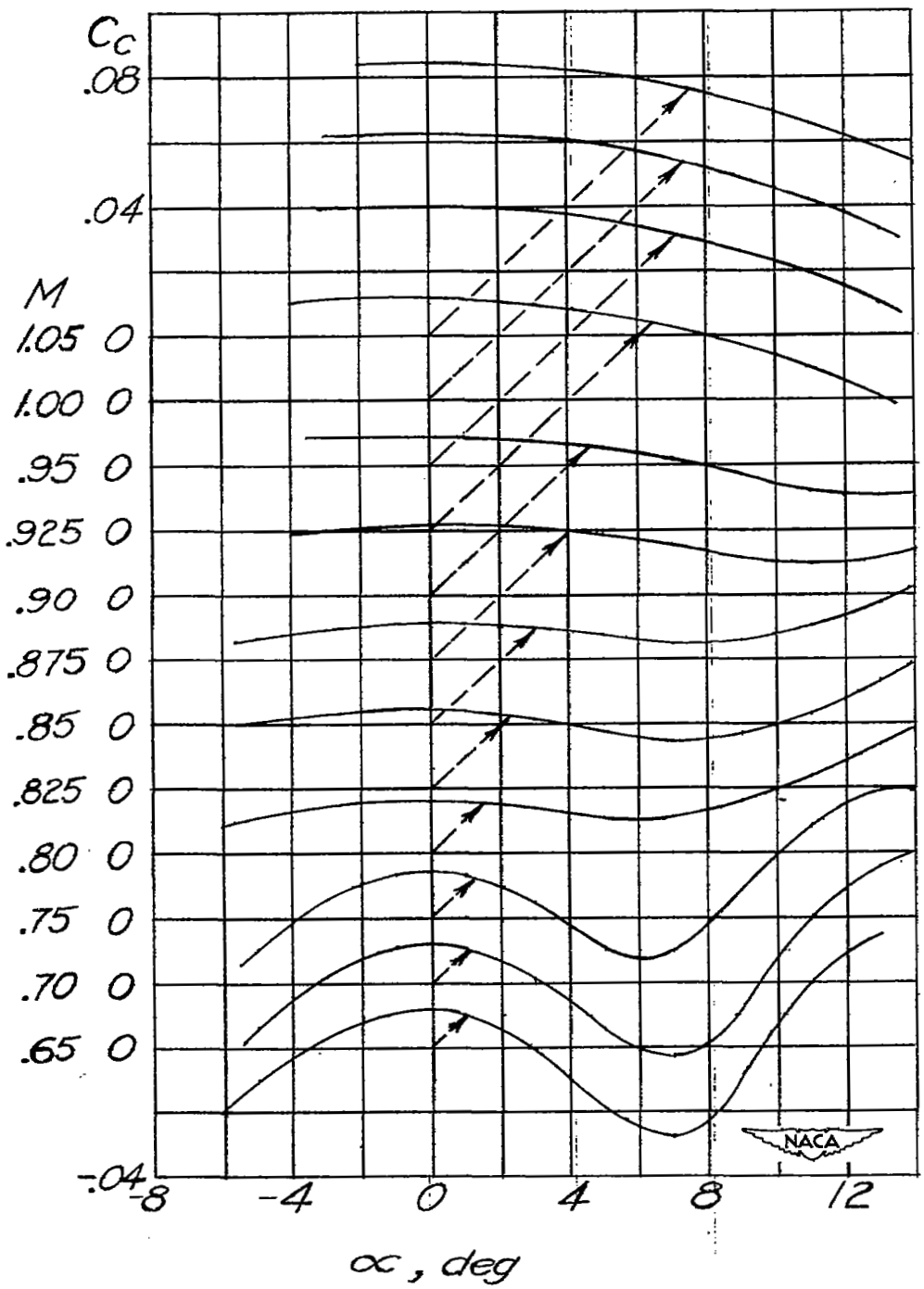

(b) Variation of chord-force coefficient with angle of attack.

Figure 6.- Concluded.

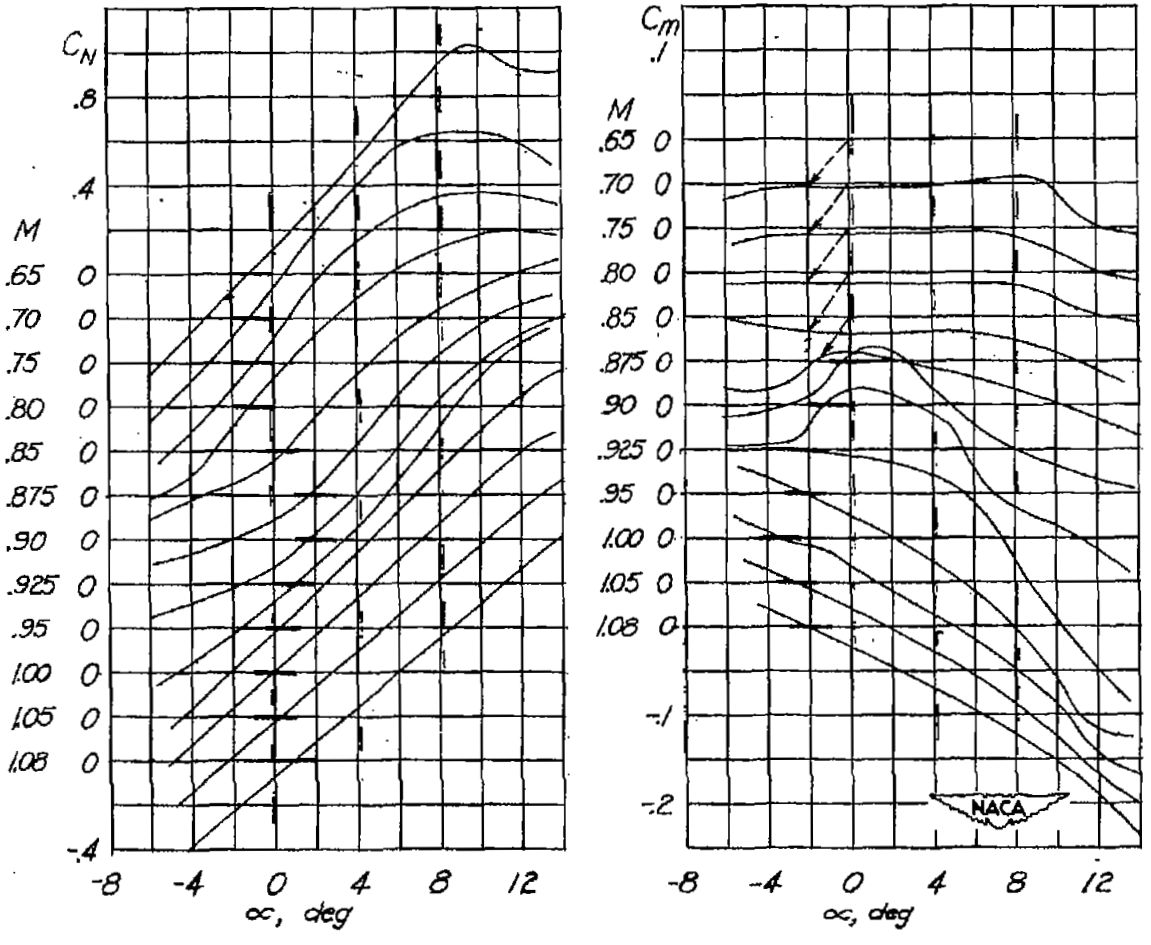

(a) Variation of normal-force and pitching-moment coefficients with angle of attack.

Figure 7.- Measured force and moment characteristics of NACA 65-210 airfoil at Mach numbers from 0.65 to 1.08.

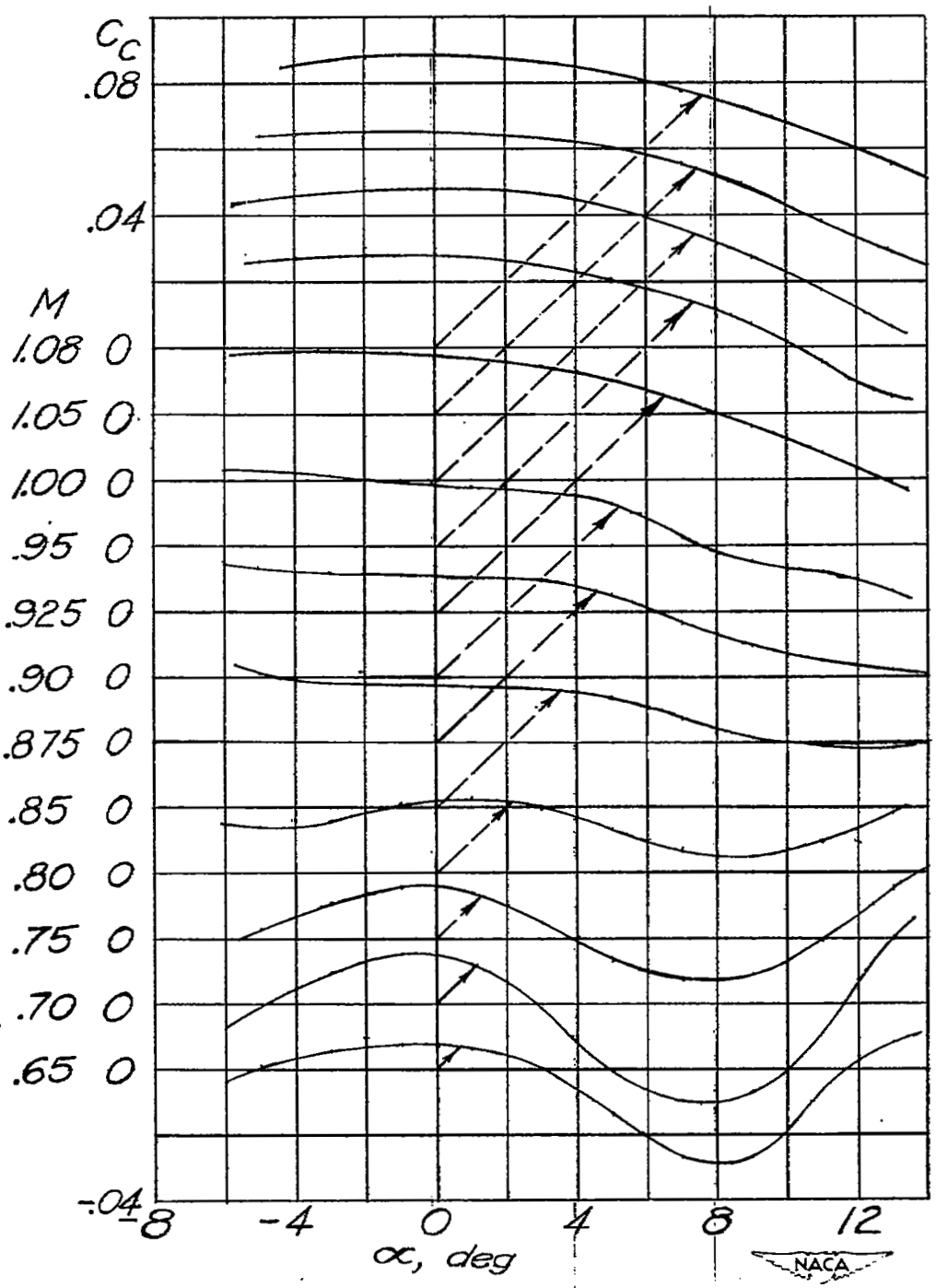

(b) Variation of chord-force coefficient with angle of attack.

Figure 7.- Concluded.

[redacted]

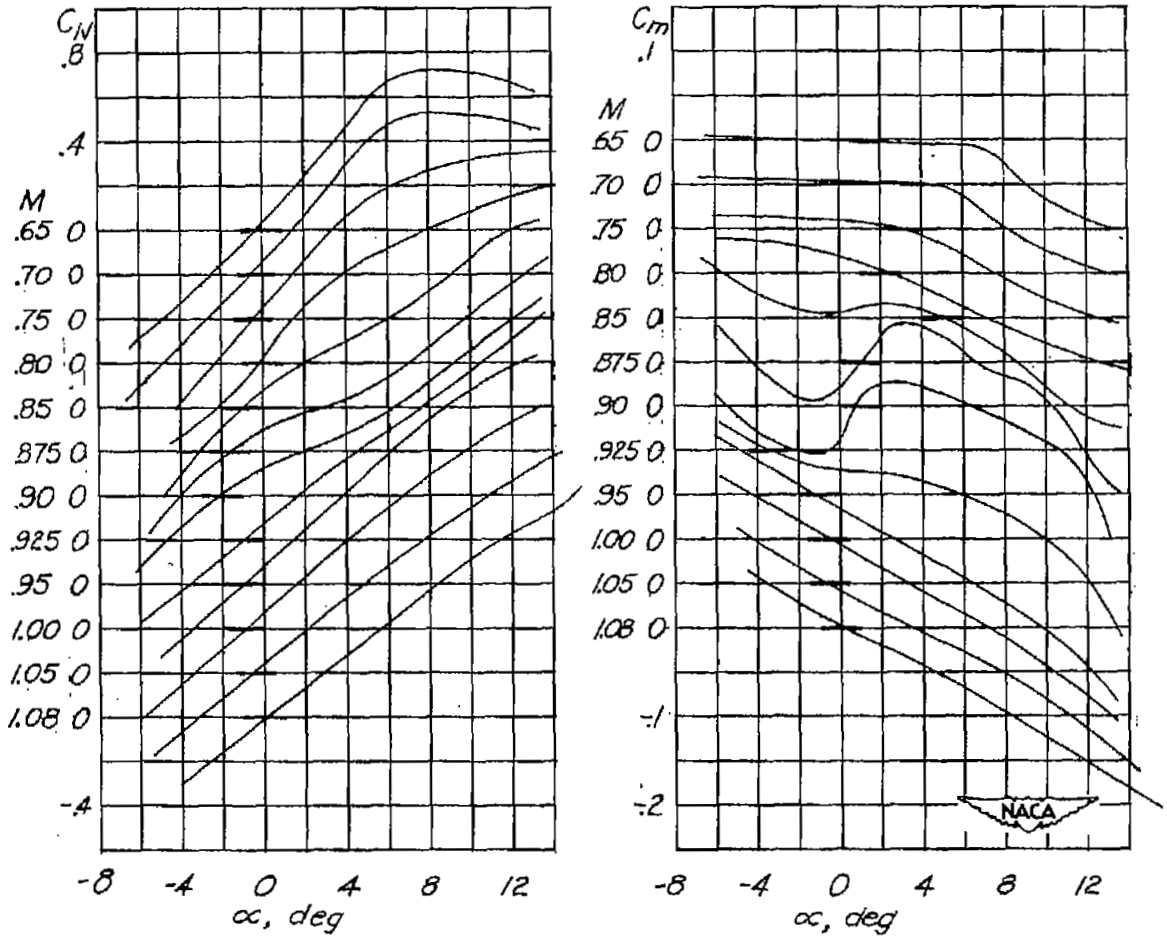

(a) Variation of normal-force and pitching-moment coefficient with angle of attack.

Figure 8.- Measured force and moment characteristics of NACA 836D110 airfoil at Mach numbers from 0.65 to 1.08.

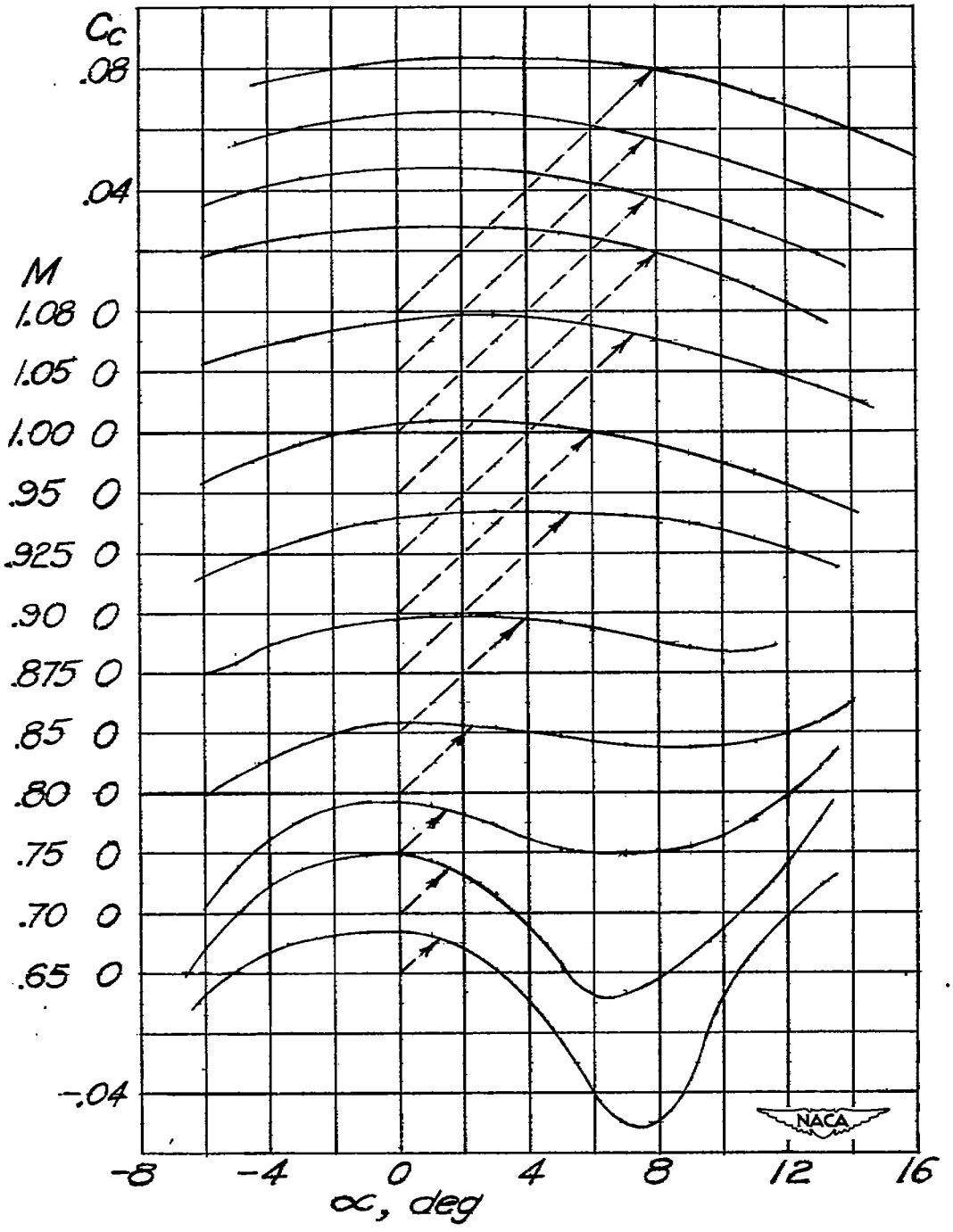

(b) Variation of chord-force coefficient with angle of attack.

Figure 8.- Concluded.

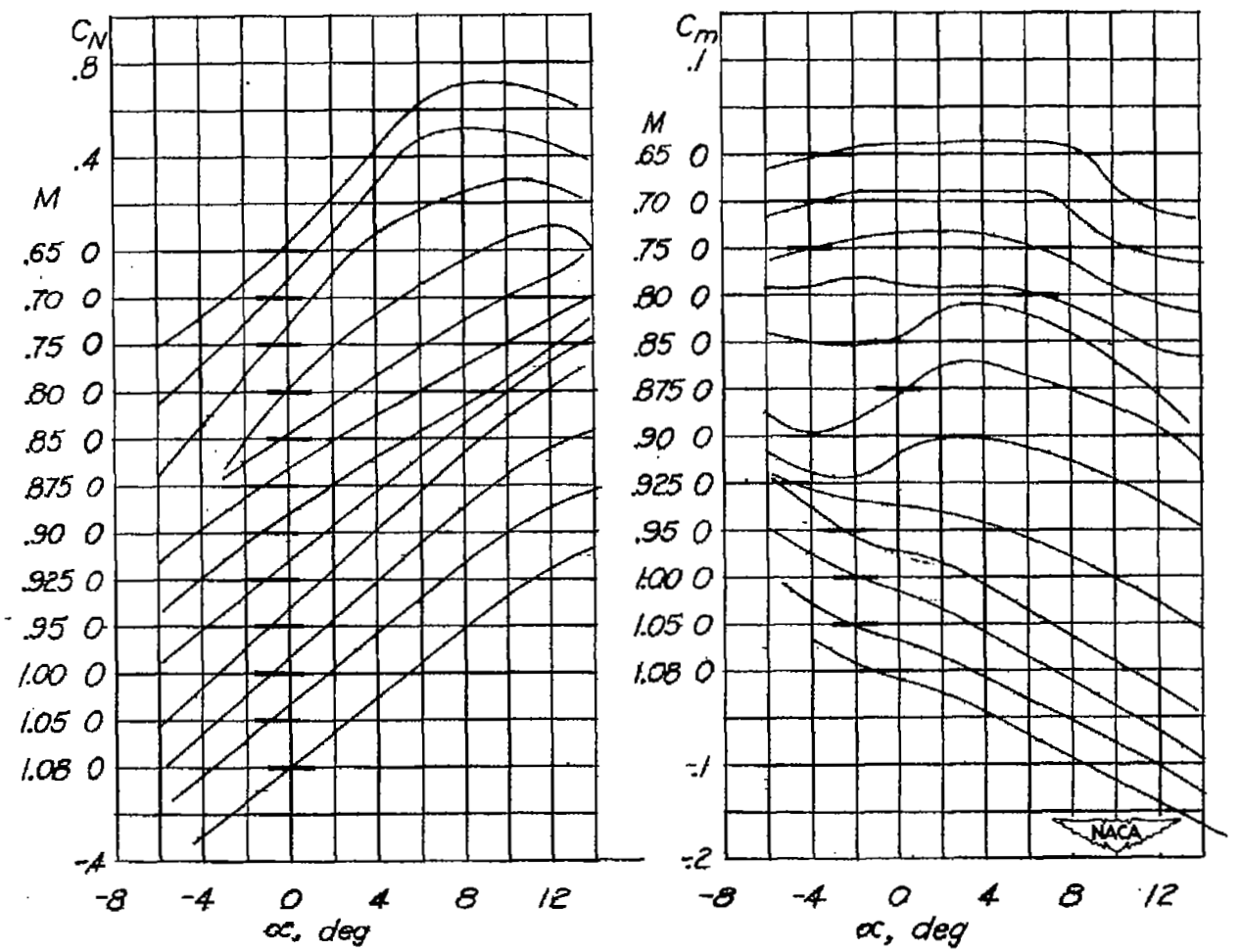

(a) Variation of normal-force and pitching-moment coefficients with angle of attack.

Figure 9.- Measured force and moment characteristics of NACA 847B110 airfoil at Mach numbers from 0.65 to 1.08.

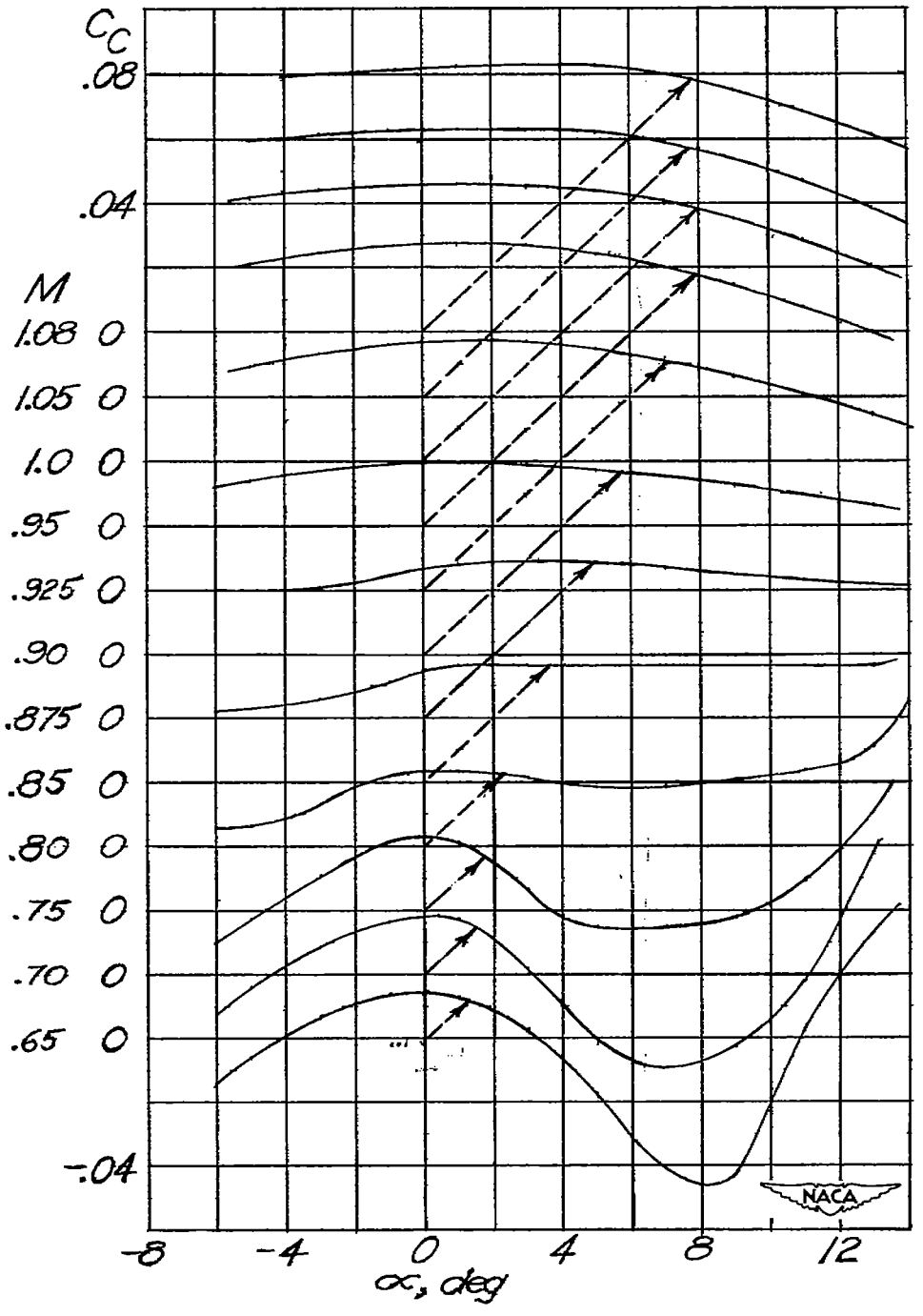

(b) Variation of chord-force coefficient with angle of attack.

Figure 9.- Concluded.

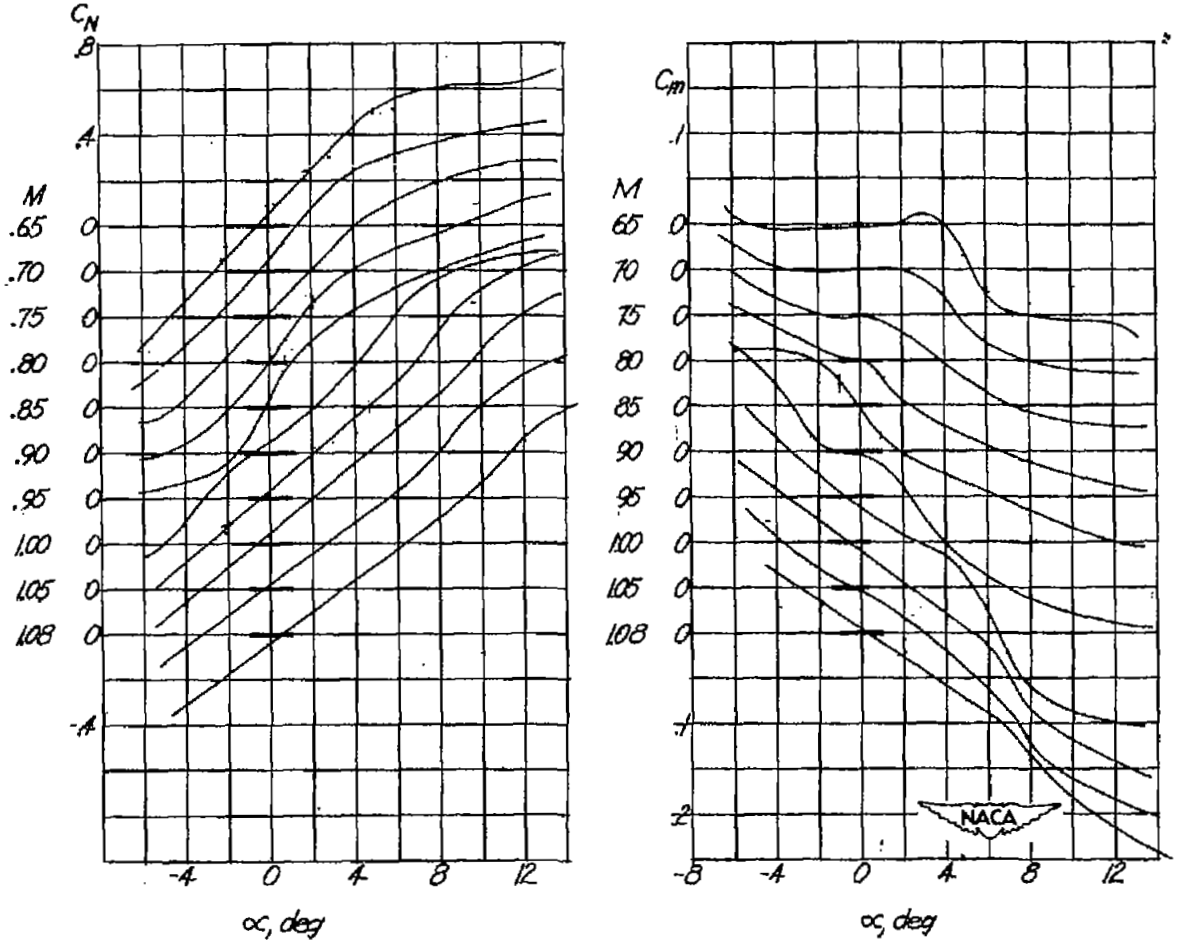

(a) Variation of normal-force and pitching-moment coefficients with angle of attack.

Figure 10.- Measured force and moment characteristics of elliptical-nosed, 10-percent-thick, uncambered airfoil at Mach numbers from 0.65 to 1.08.

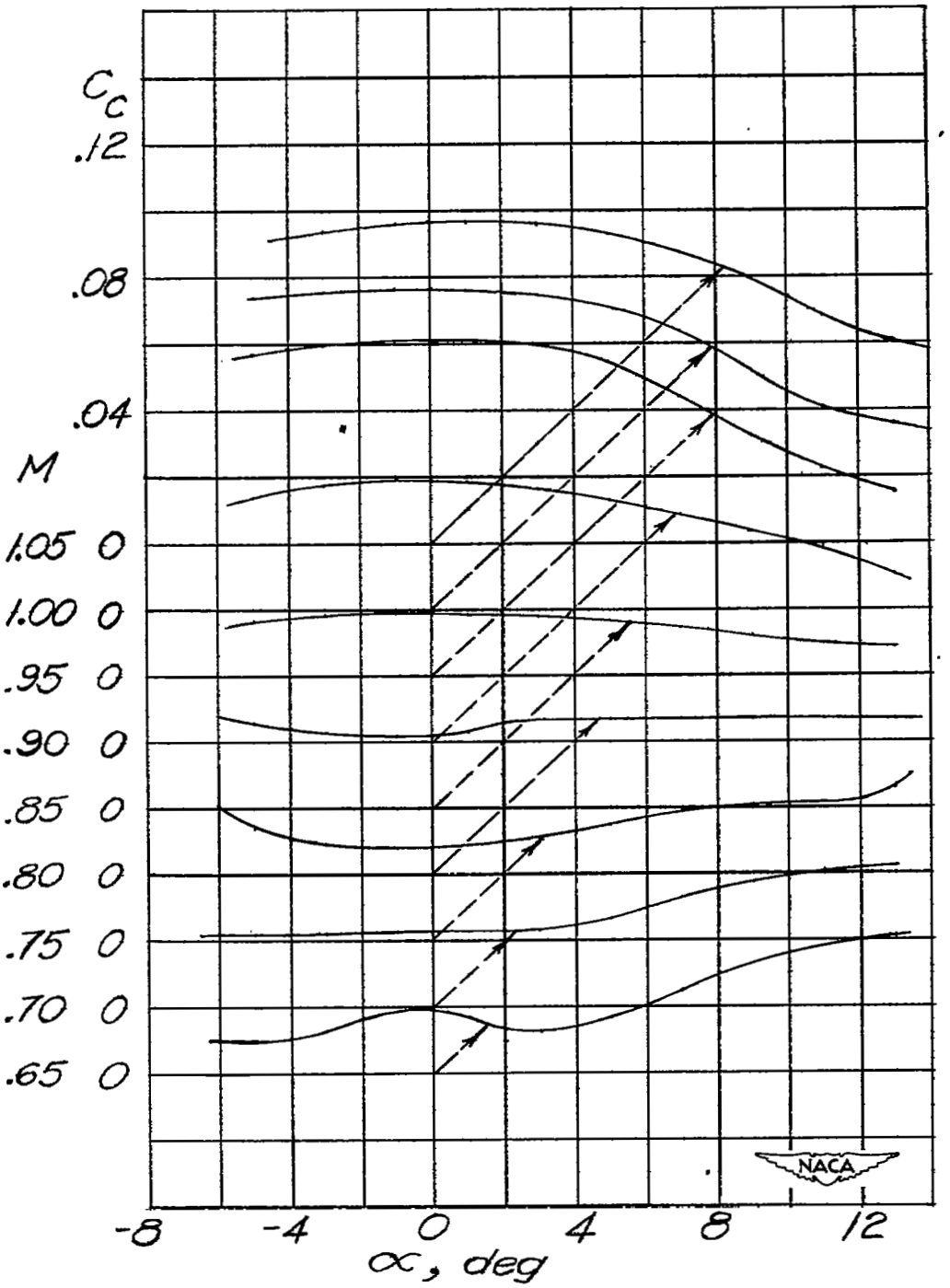

(b) Variation of chord-force coefficient with angle of attack.

Figure 10.- Concluded.

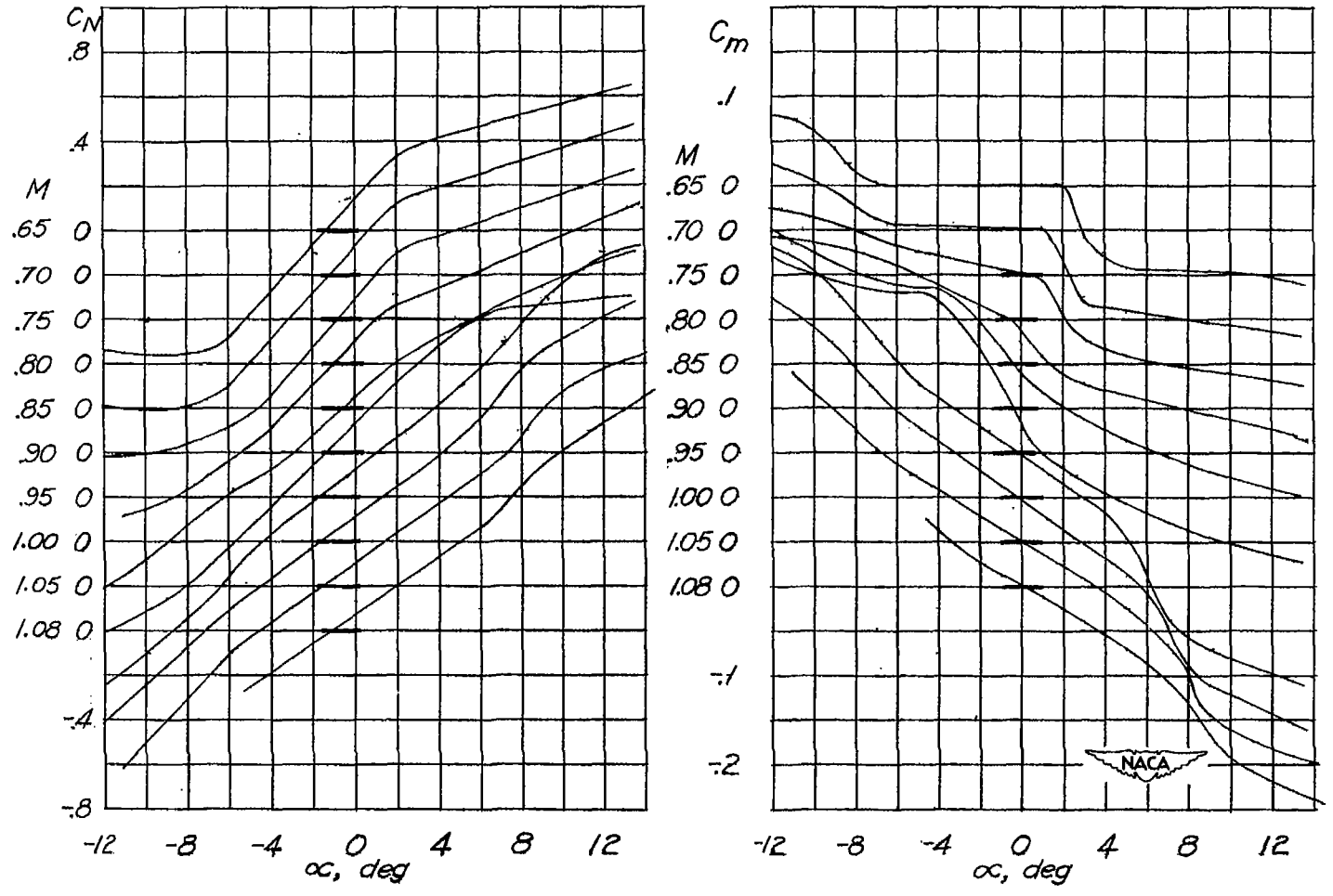

(a) Variation of normal-force and pitching-moment coefficients with angle of attack.

Figure 11.- Measured force and moment characteristics of elliptical-nosed, 10-percent-thick, reflex-cambered airfoil at Mach numbers from 0.65 to 1.08.

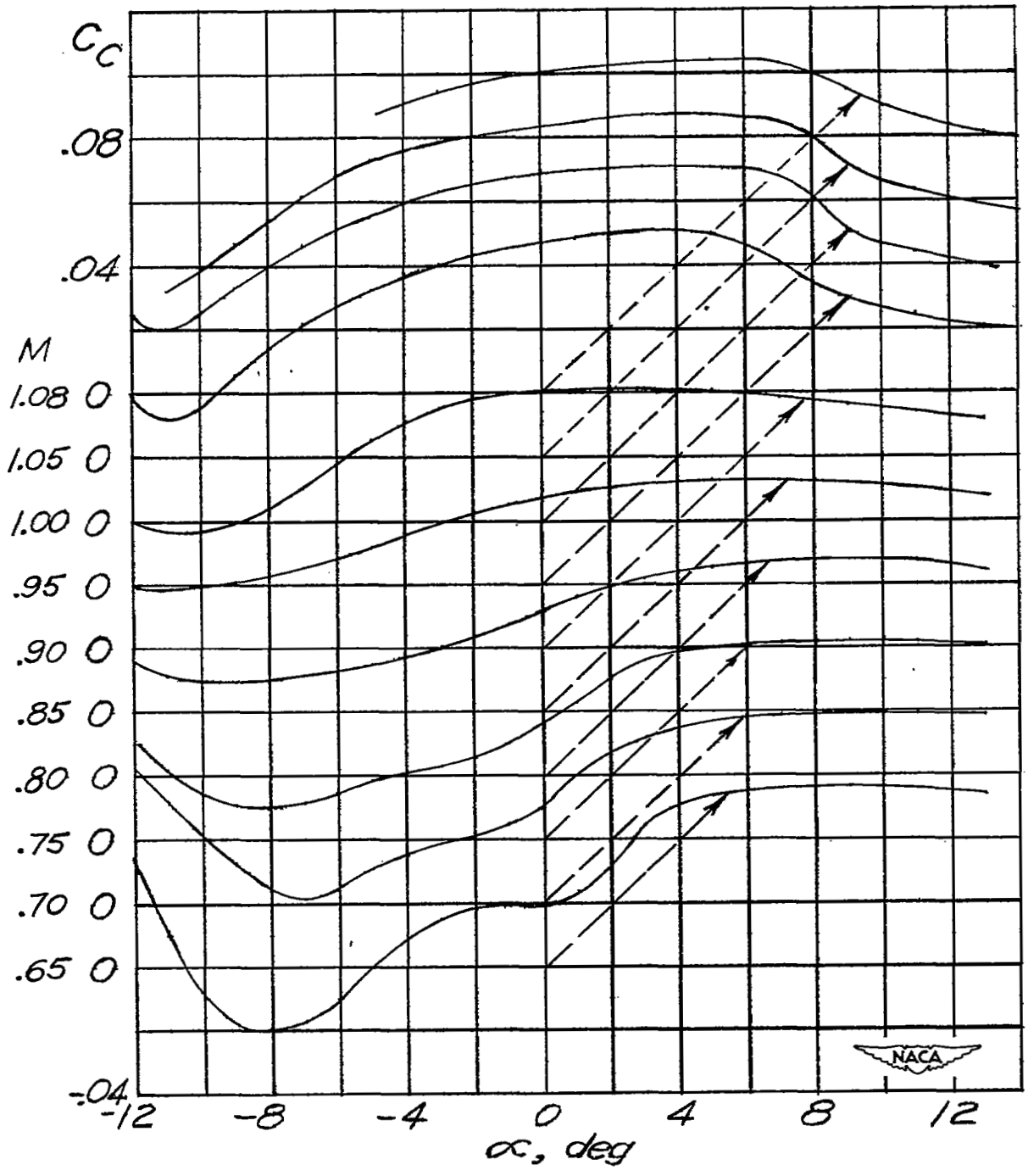

(b) Variation of chord-force coefficient with angle of attack.

Figure 11.- Concluded.

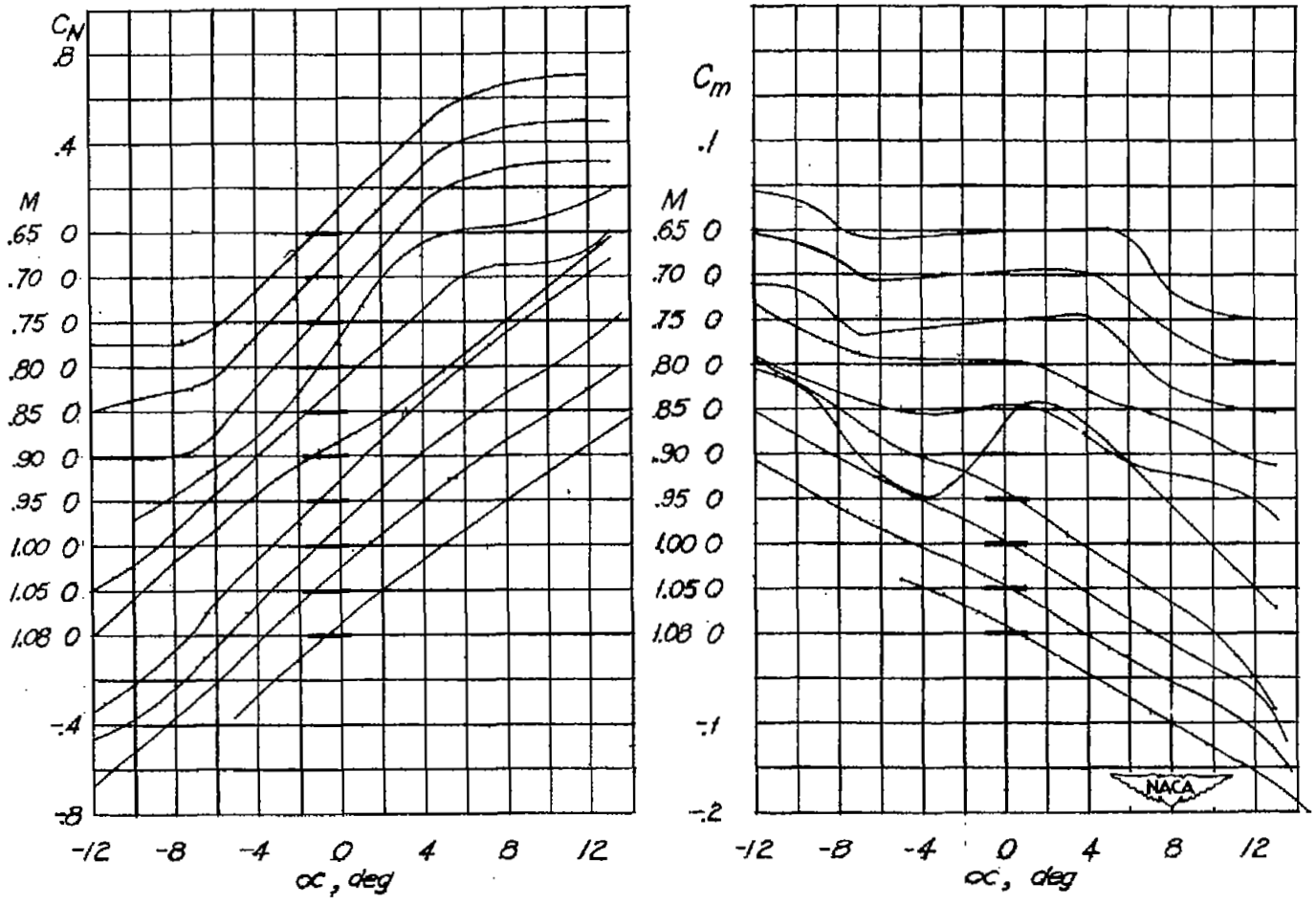

(a) Variation of normal-force and pitching-moment coefficient with angle of attack.

Figure 12.- Measured force and moment characteristics of an airfoil having a nominal thickness distribution of the NACA 65-010 airfoil and a reflexed-camber line at Mach numbers 0.65 to 1.08.

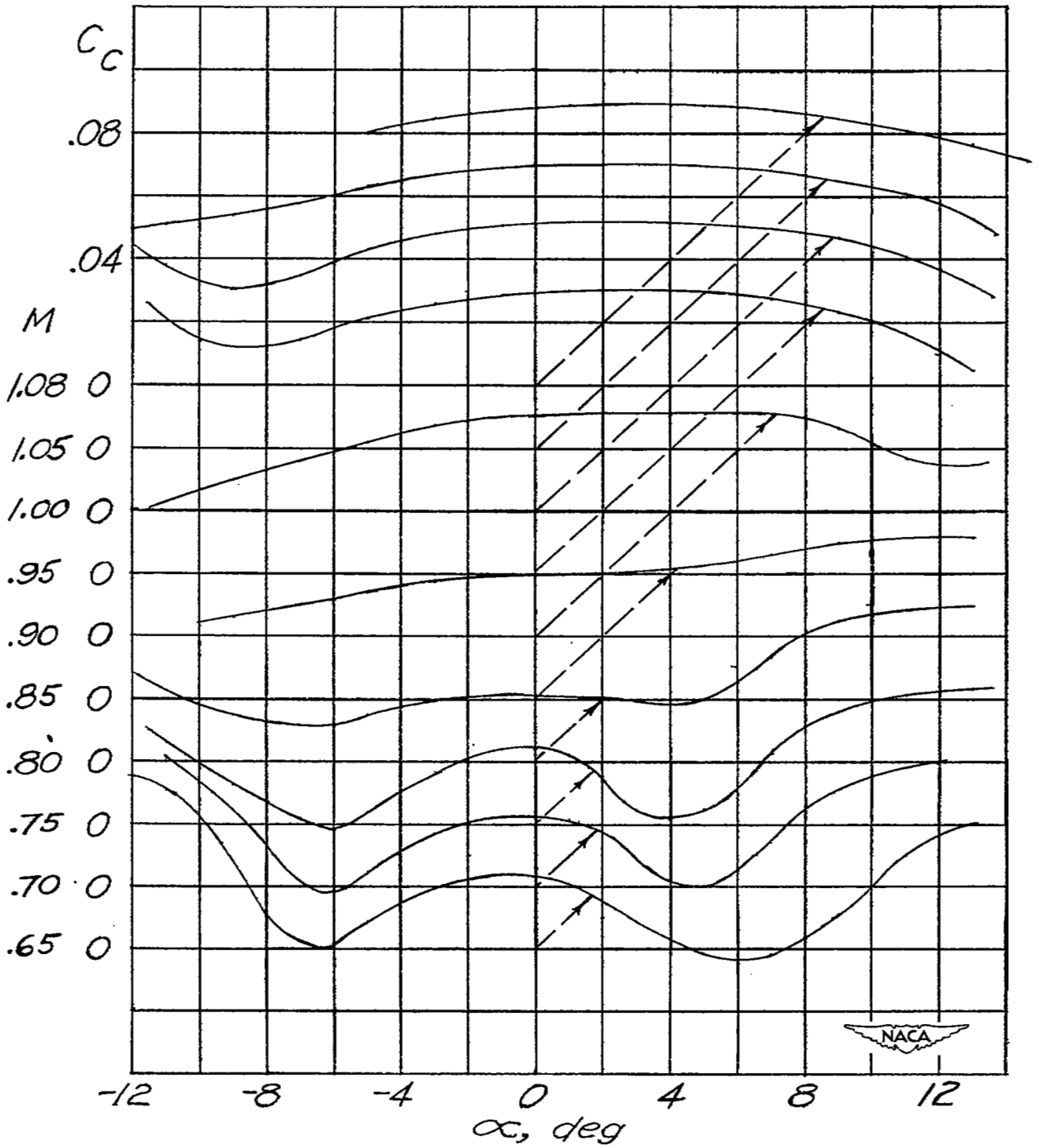

(b) Variation of chord-force coefficient with angle of attack.

Figure 12.- Concluded.

[redacted]

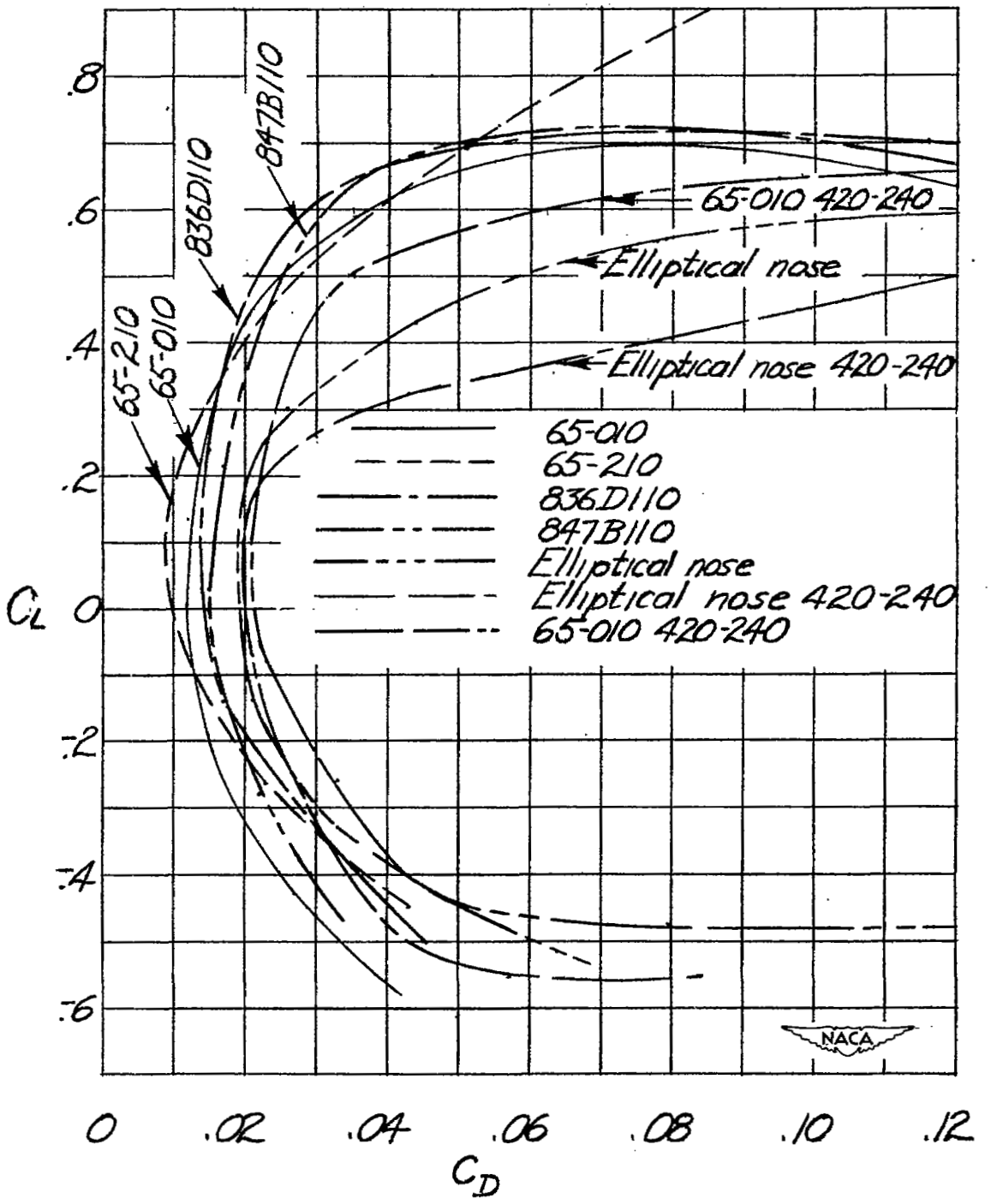

(a) M = 0.65.

Figure 13.- Lift-drag polars of the seven test airfoils.

[redacted]

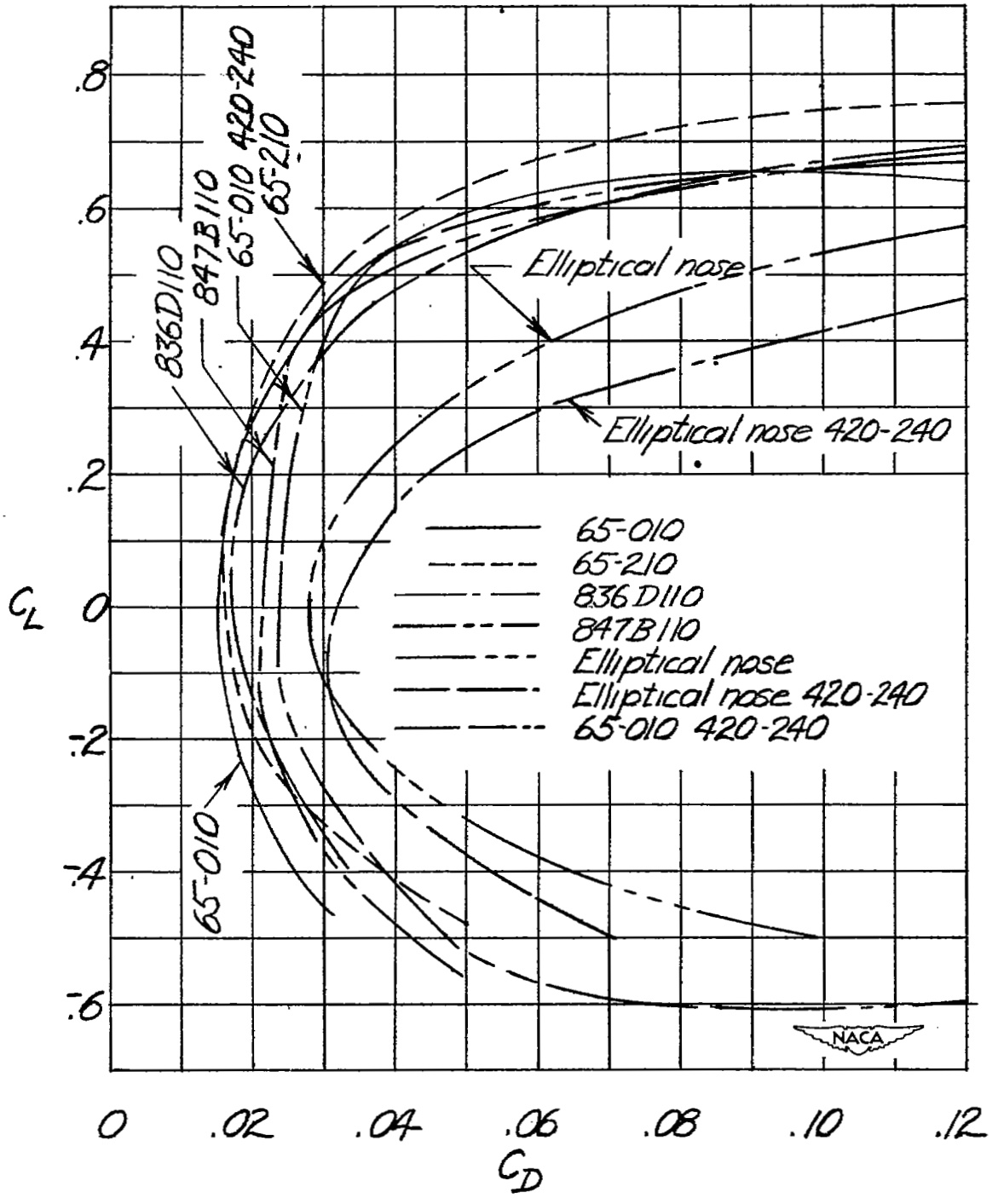

(b) M = 0.75.

Figure 13.- Continued.

[redacted]

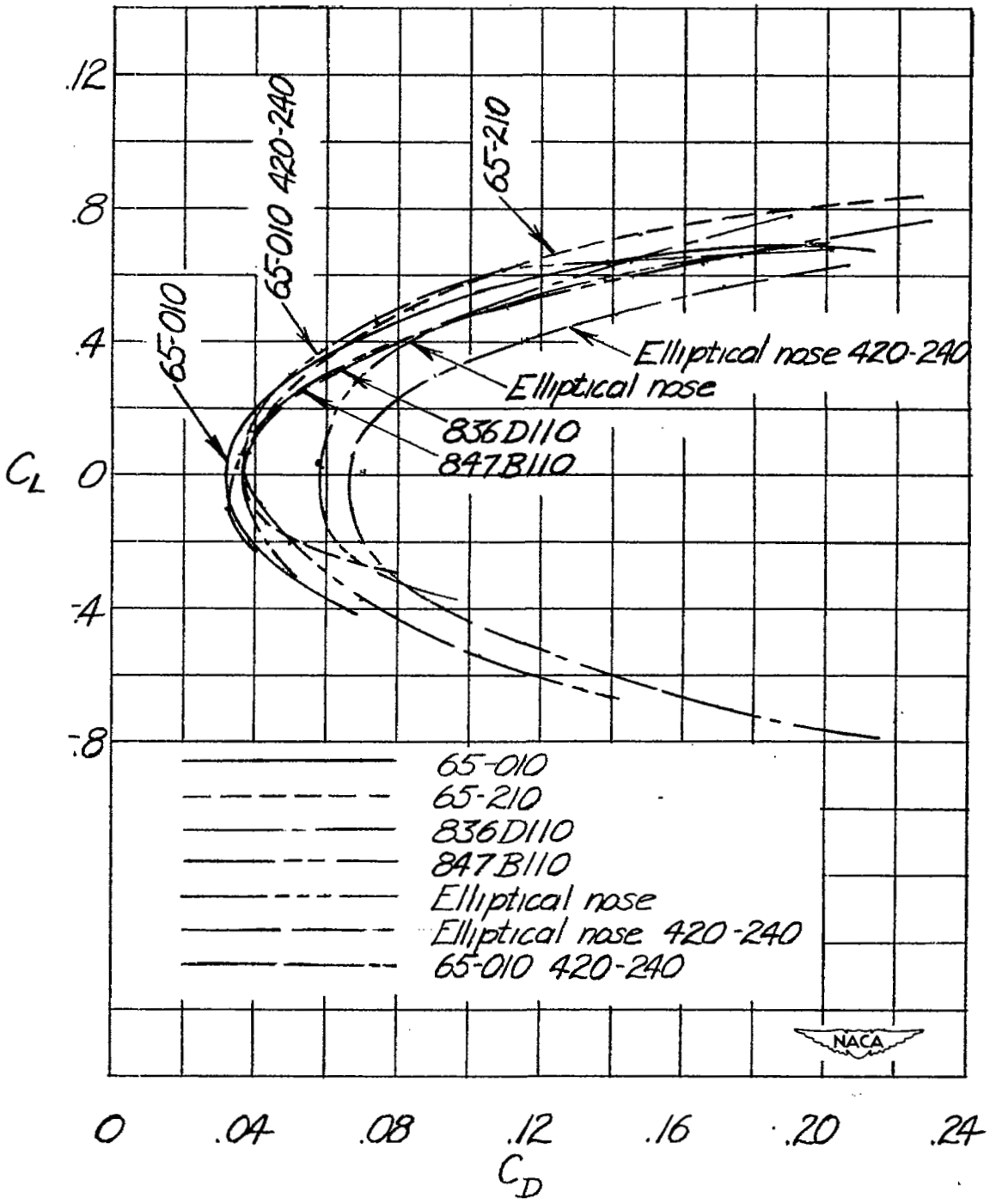

(c) M = 0.85.

Figure 13.- Continued.

[redacted]

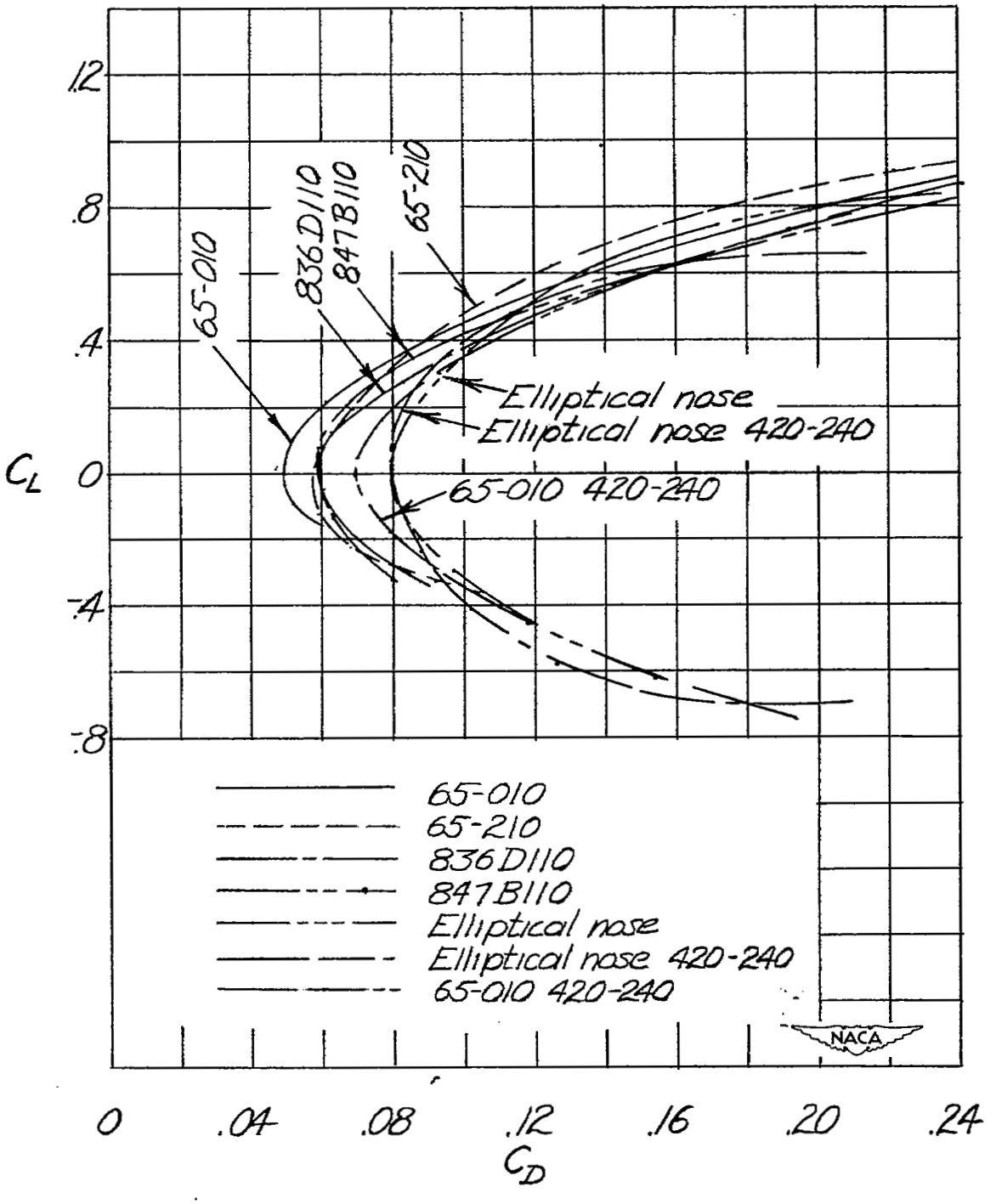

(d) M = 0.90.

Figure 13.- Continued.

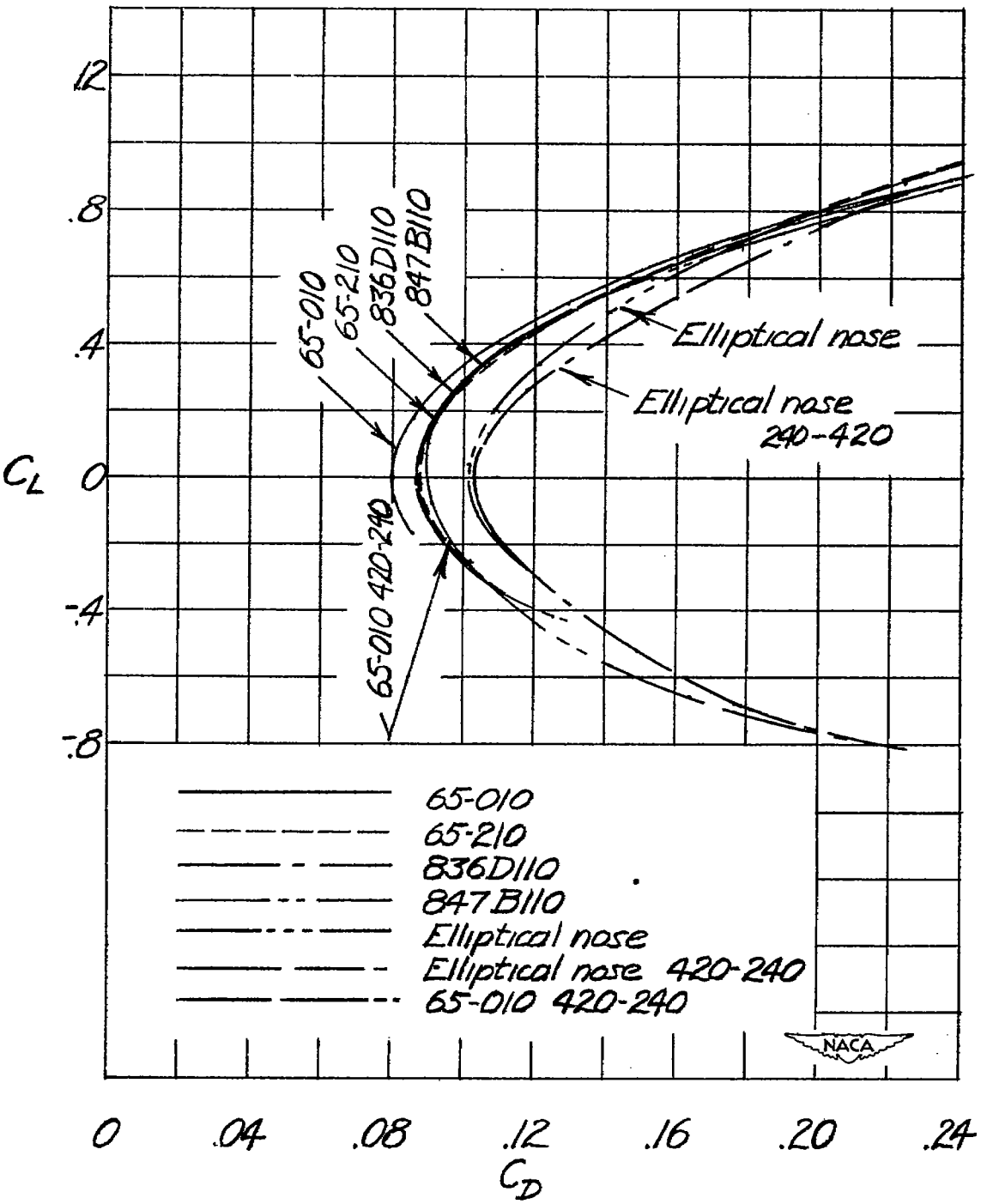

(e) M = 0.95.

Figure 13.- Continued.

[redacted]

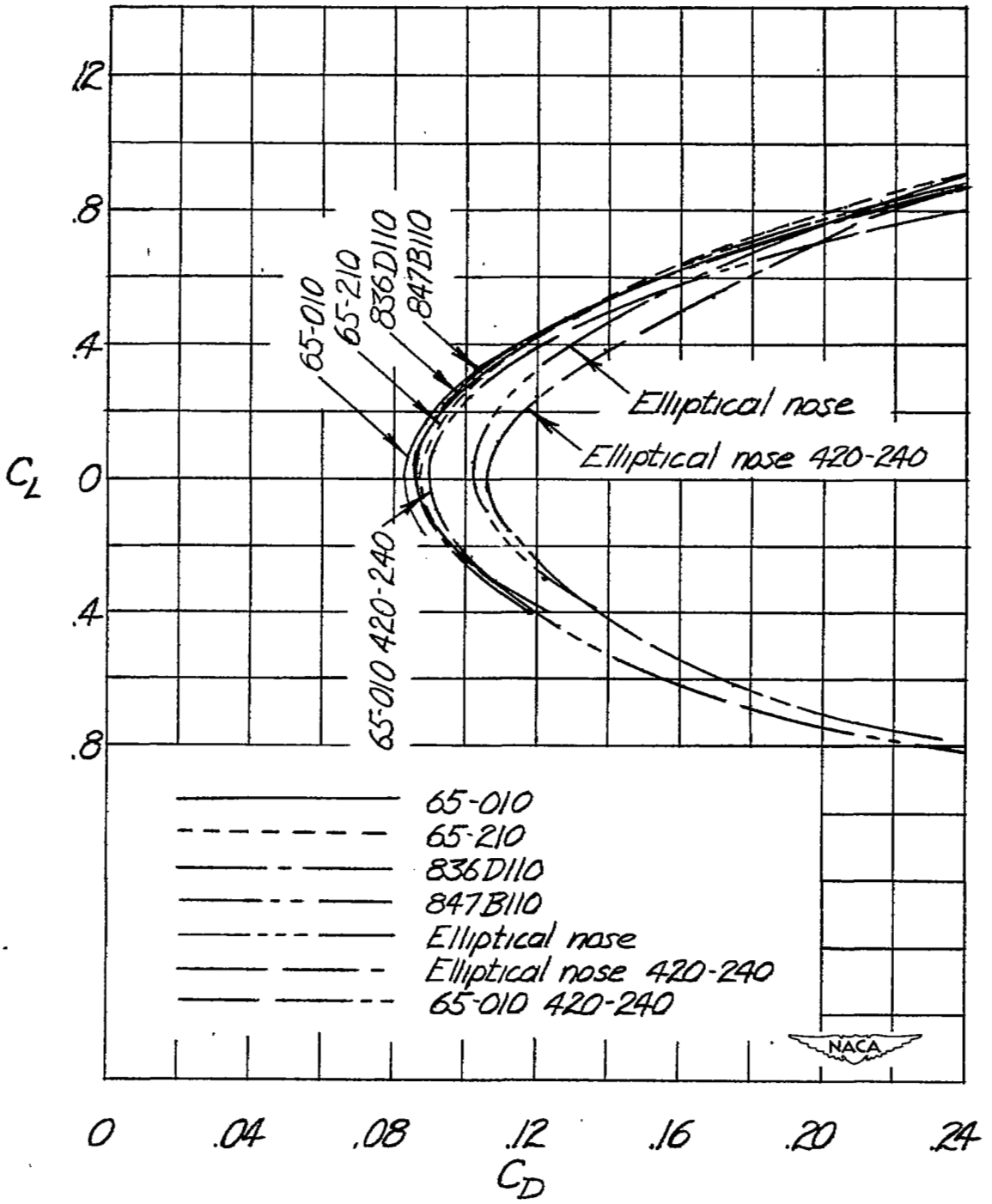

(f) M = 1.00.

Figure 13.- Continued.

[redacted]

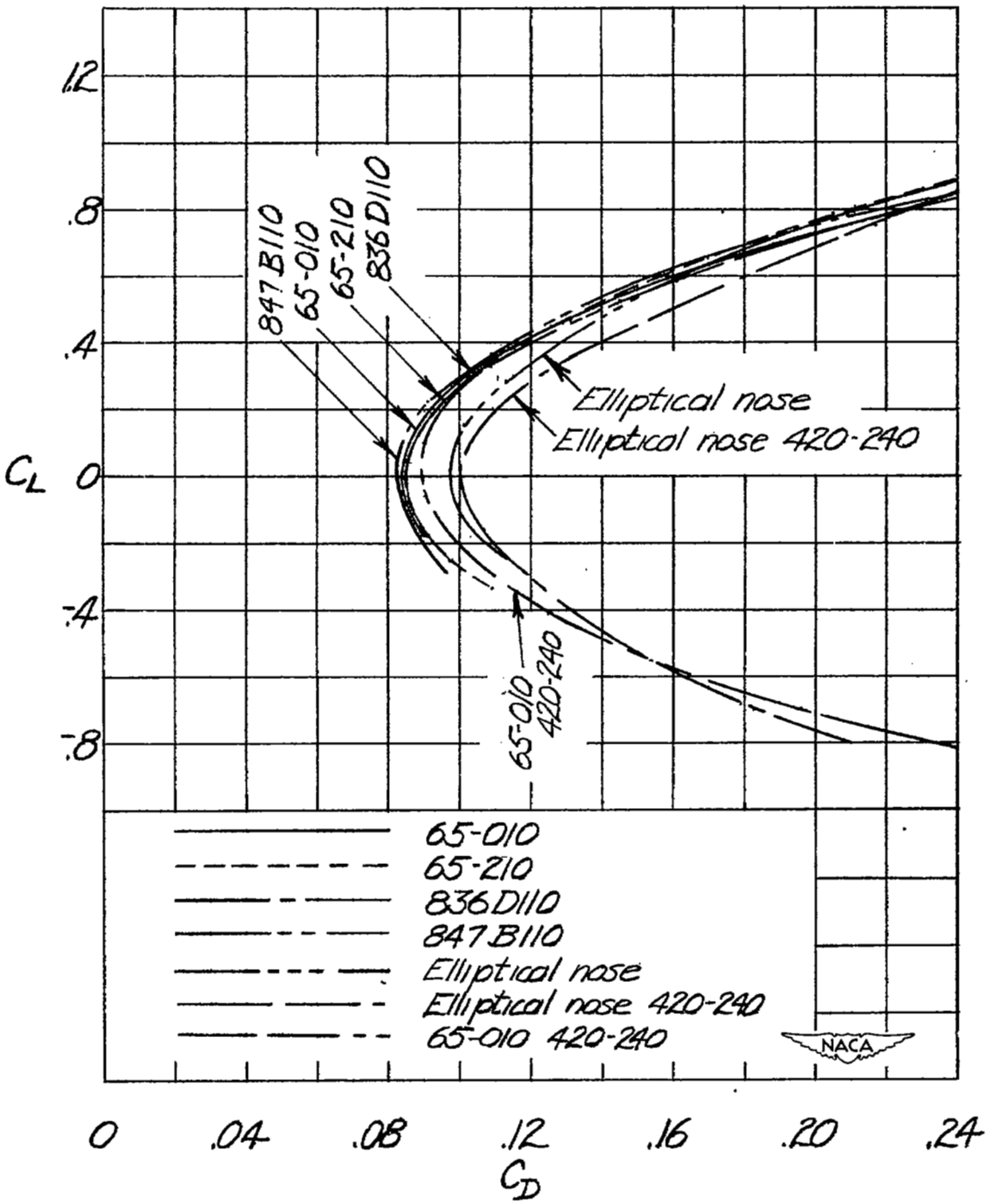

(g) M = 1.05.

Figure 13.- Continued.

[redacted]

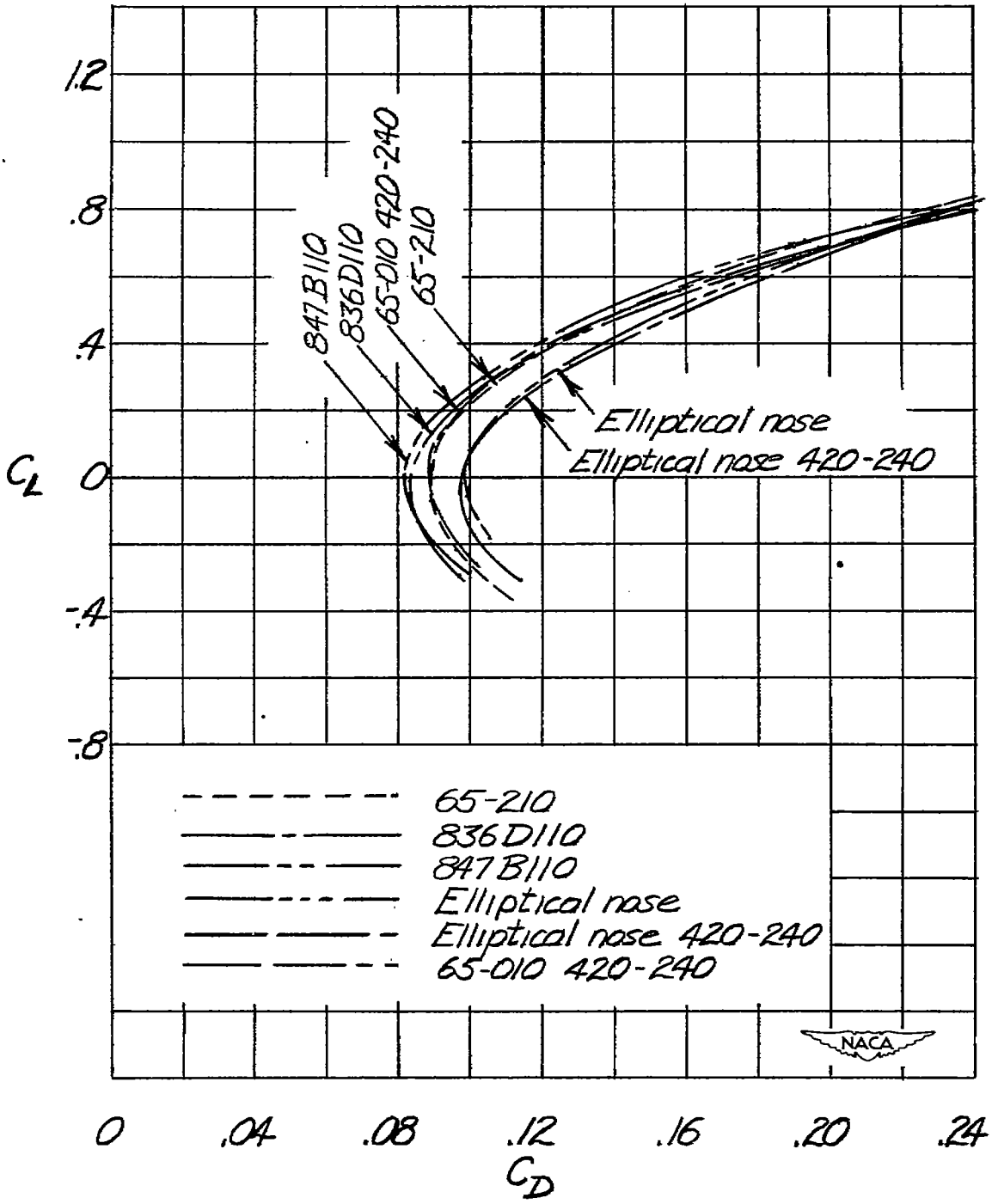

(h) M = 1.08.

Figure 13.- Concluded.

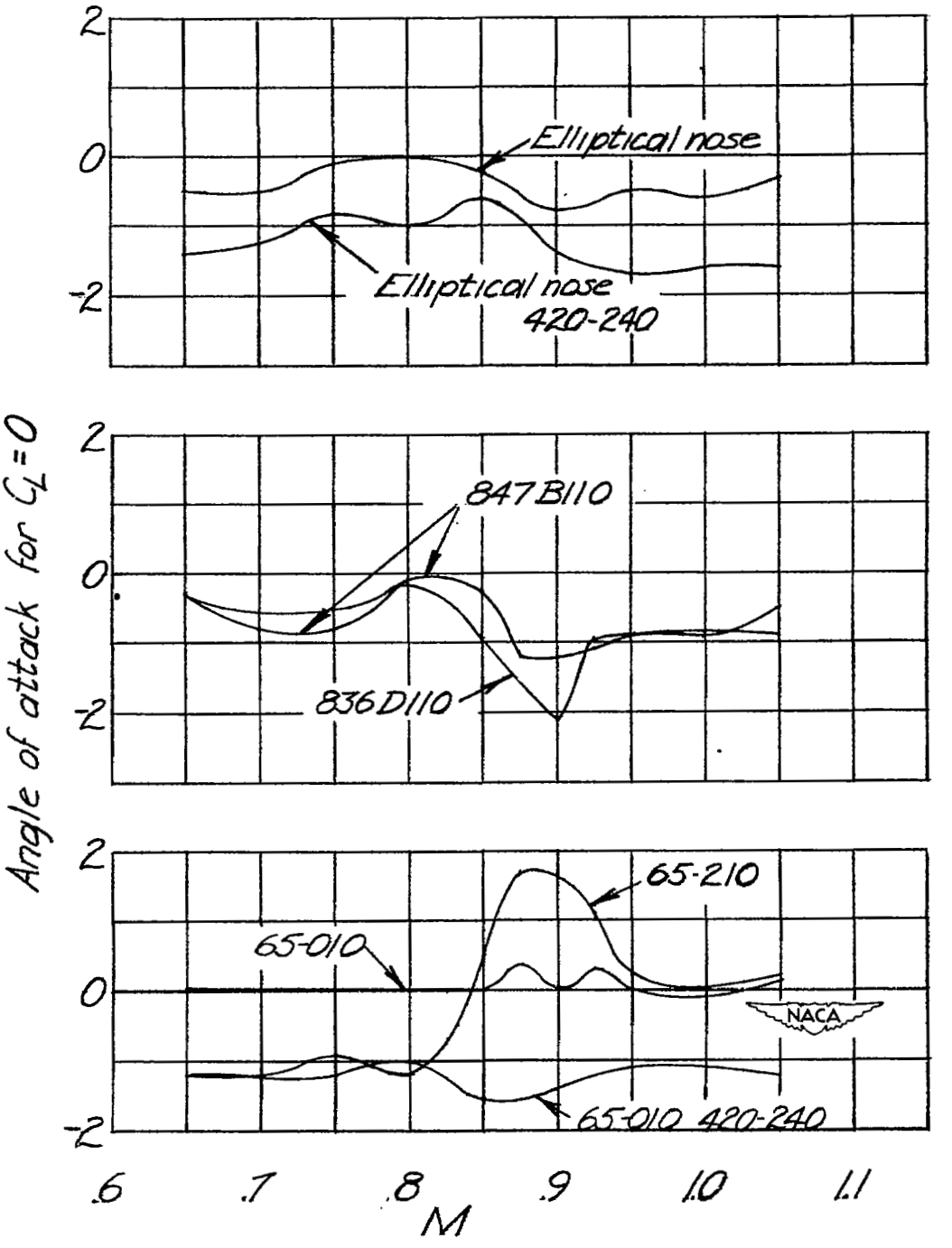

(a) $C_L = 0$.

Figure 14.- Variation with Mach number of angle of attack required for various values of C_L for the seven test airfoils.

[redacted]

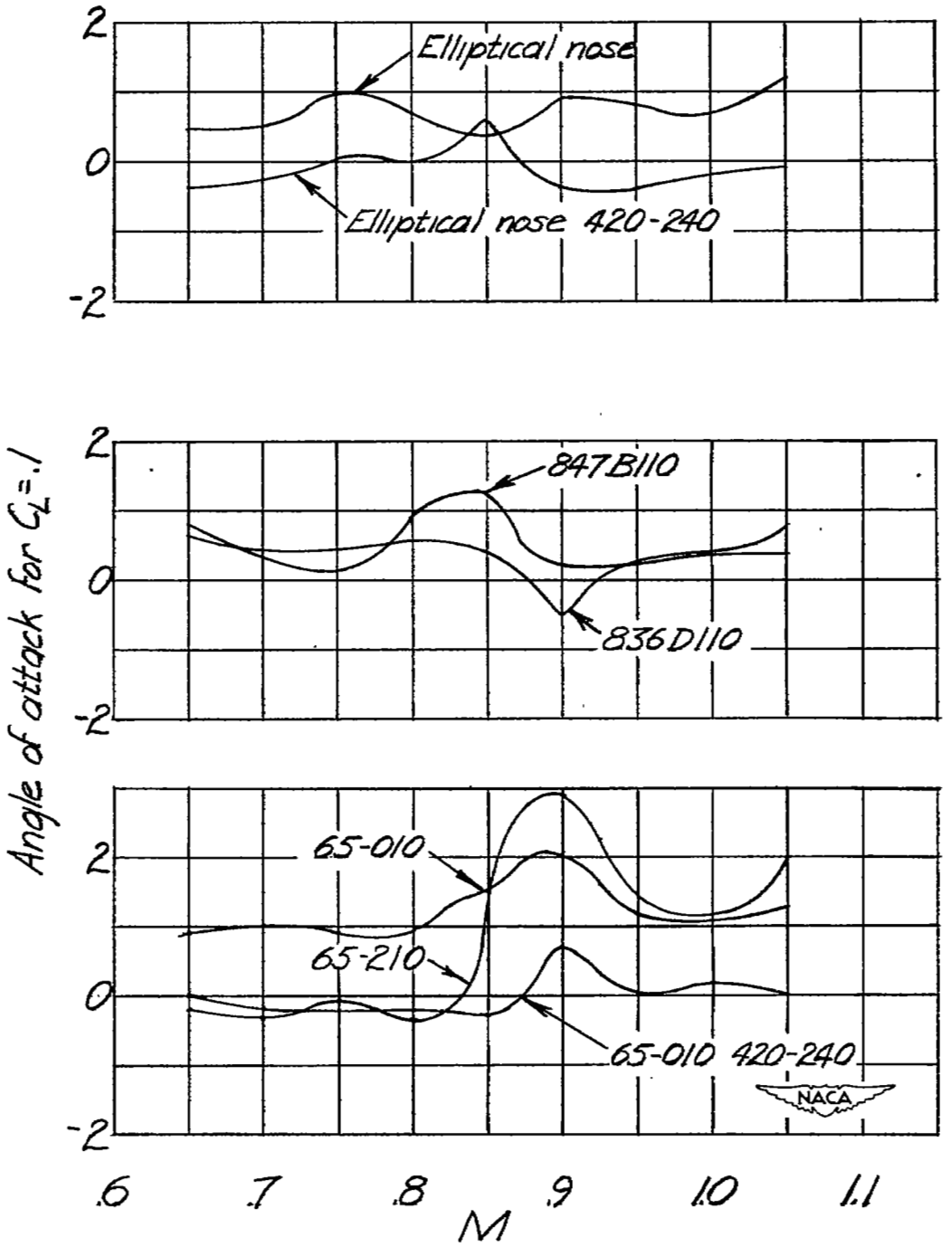

(b) C_L = 0.1.

Figure 14.- Continued.

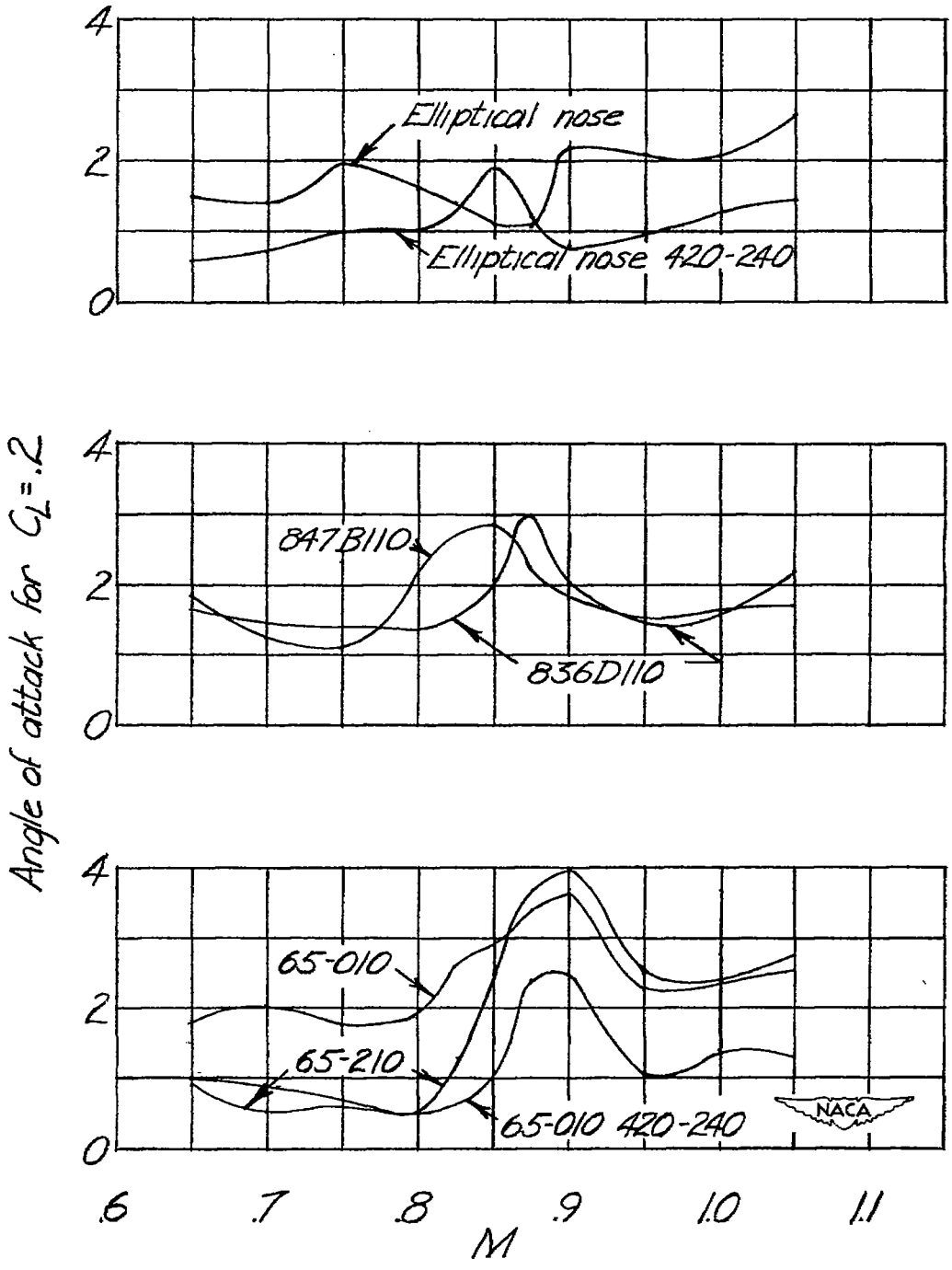

(c) $C_L = 0.2$.

Figure 14.- Continued.

[redacted]

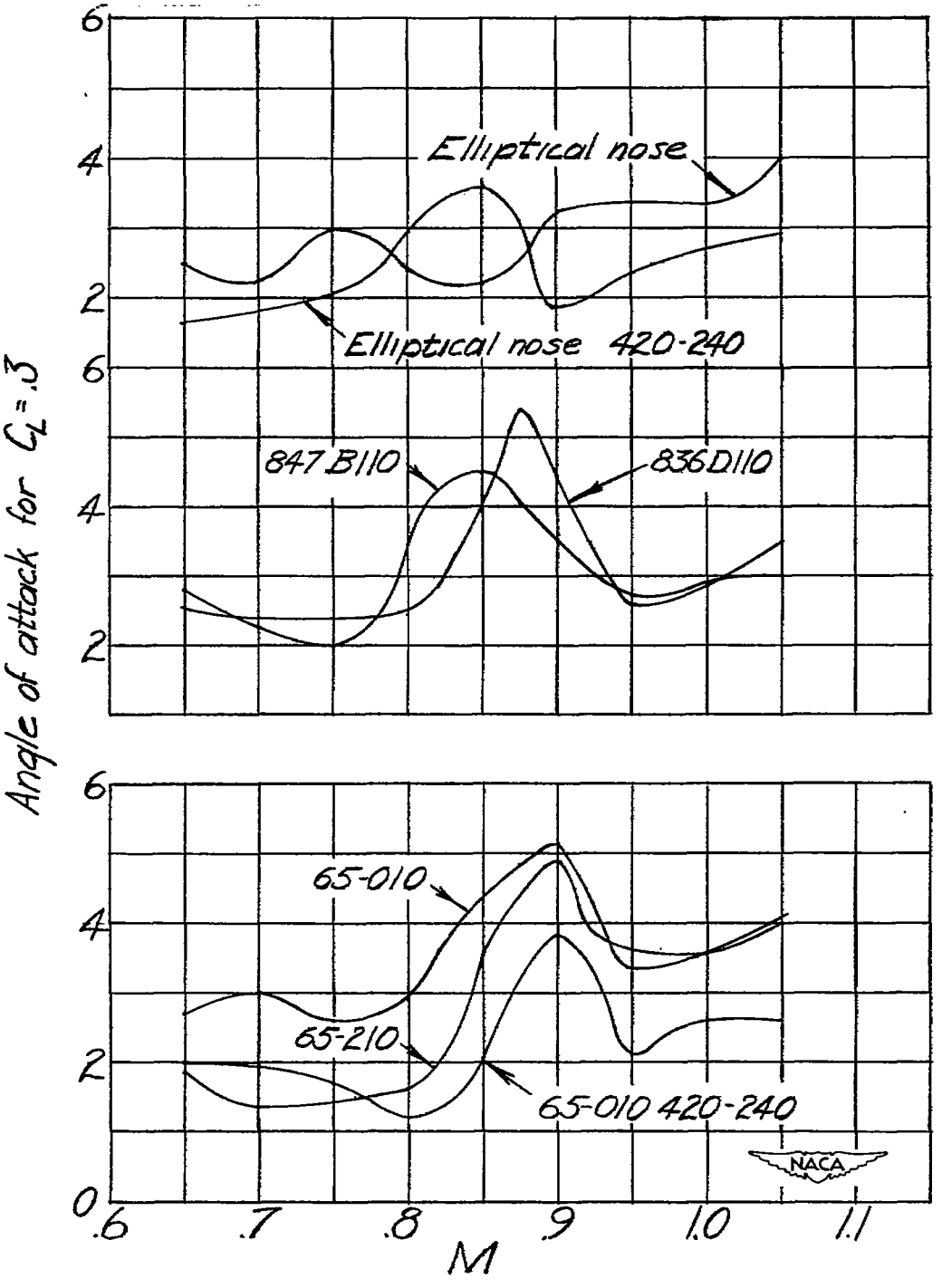

(d) $C_L = 0.3$.

Figure 14.- Concluded.

[redacted]

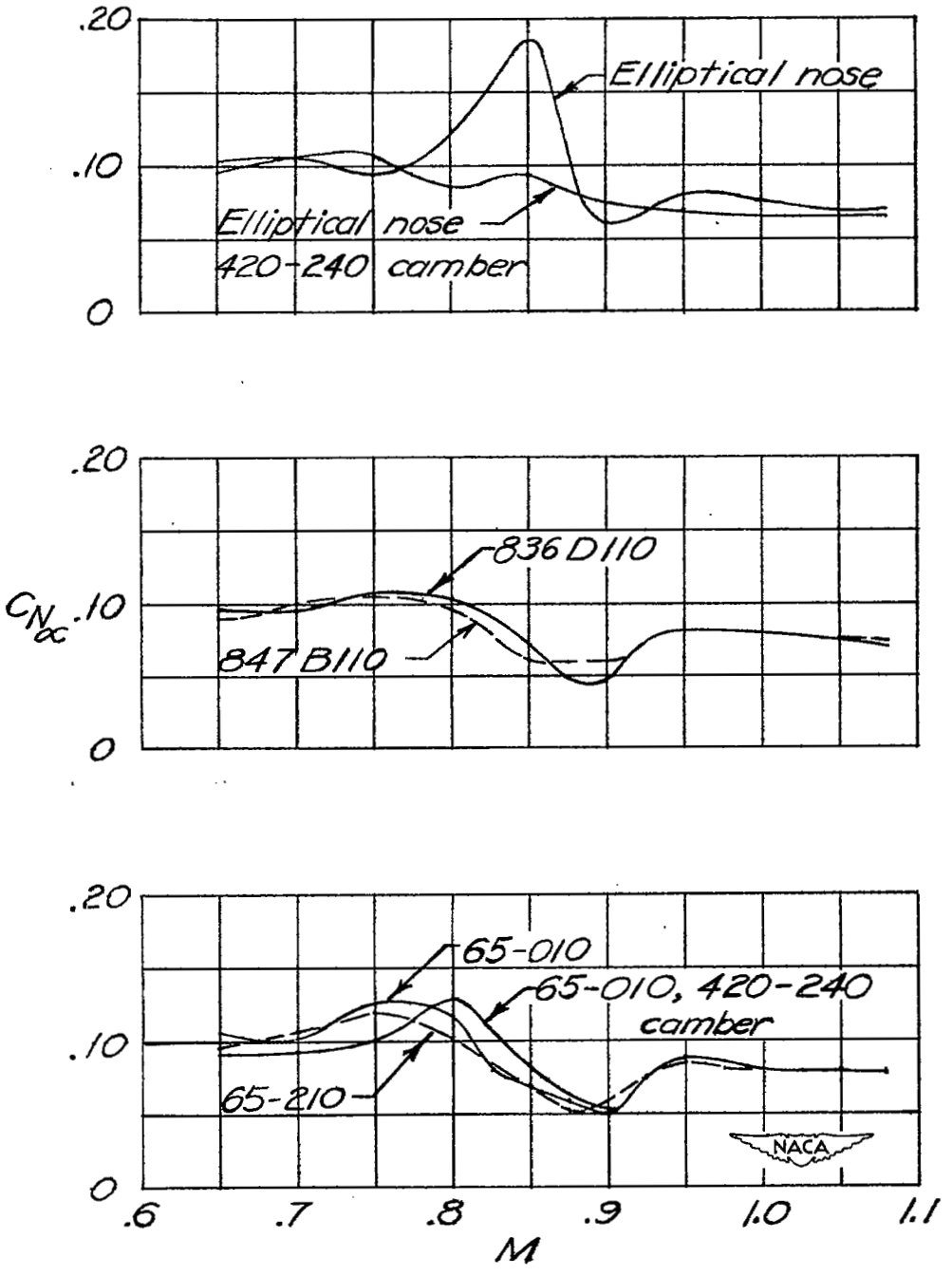

(a) $\alpha = 0^\circ$.

Figure 15.- Variation of the normal-force-curve slope C_{N_α} with Mach number at two different angles of attack for the seven test airfoils.

[redacted]

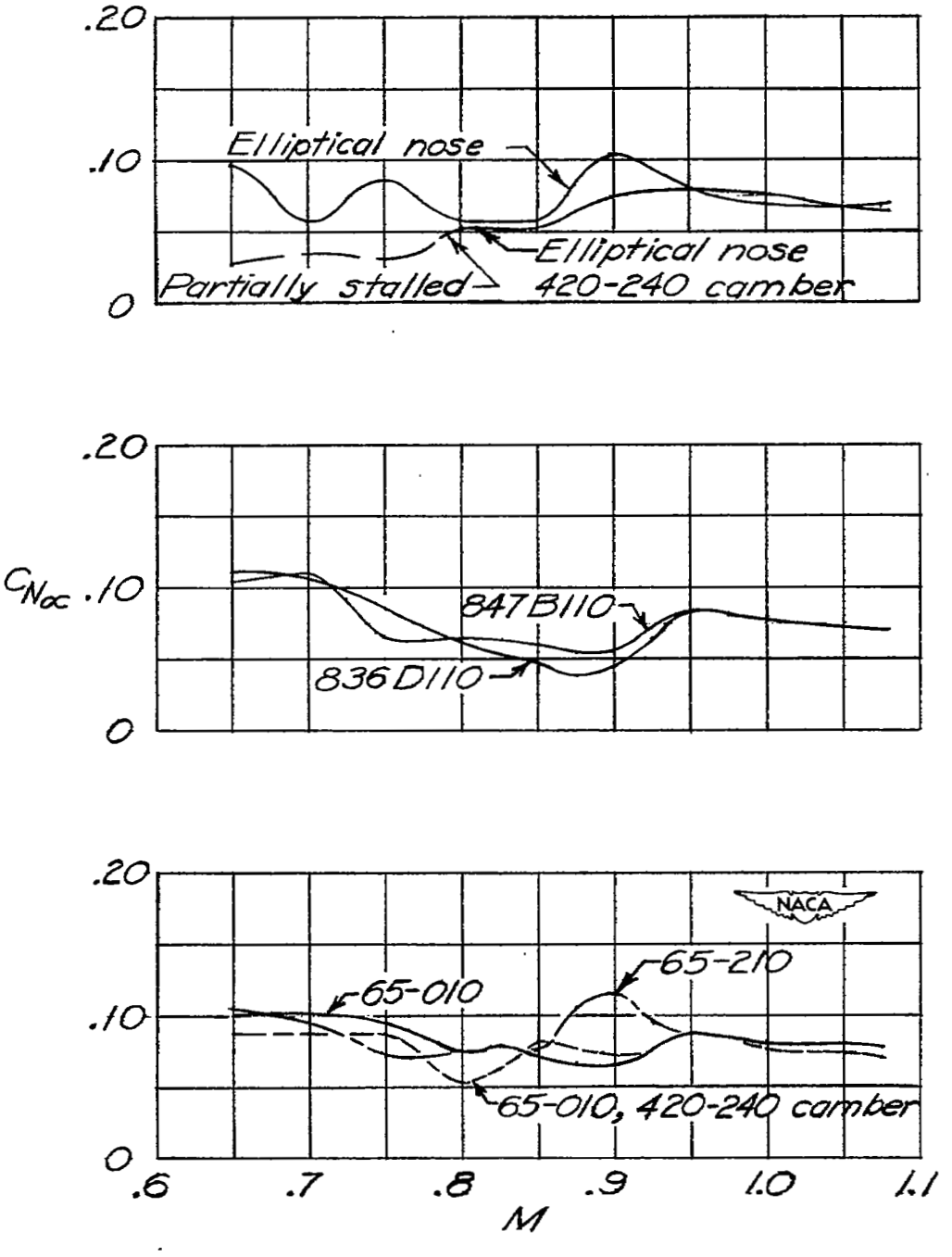

(b) $\alpha = 4^\circ$.

Figure 15.- Concluded.

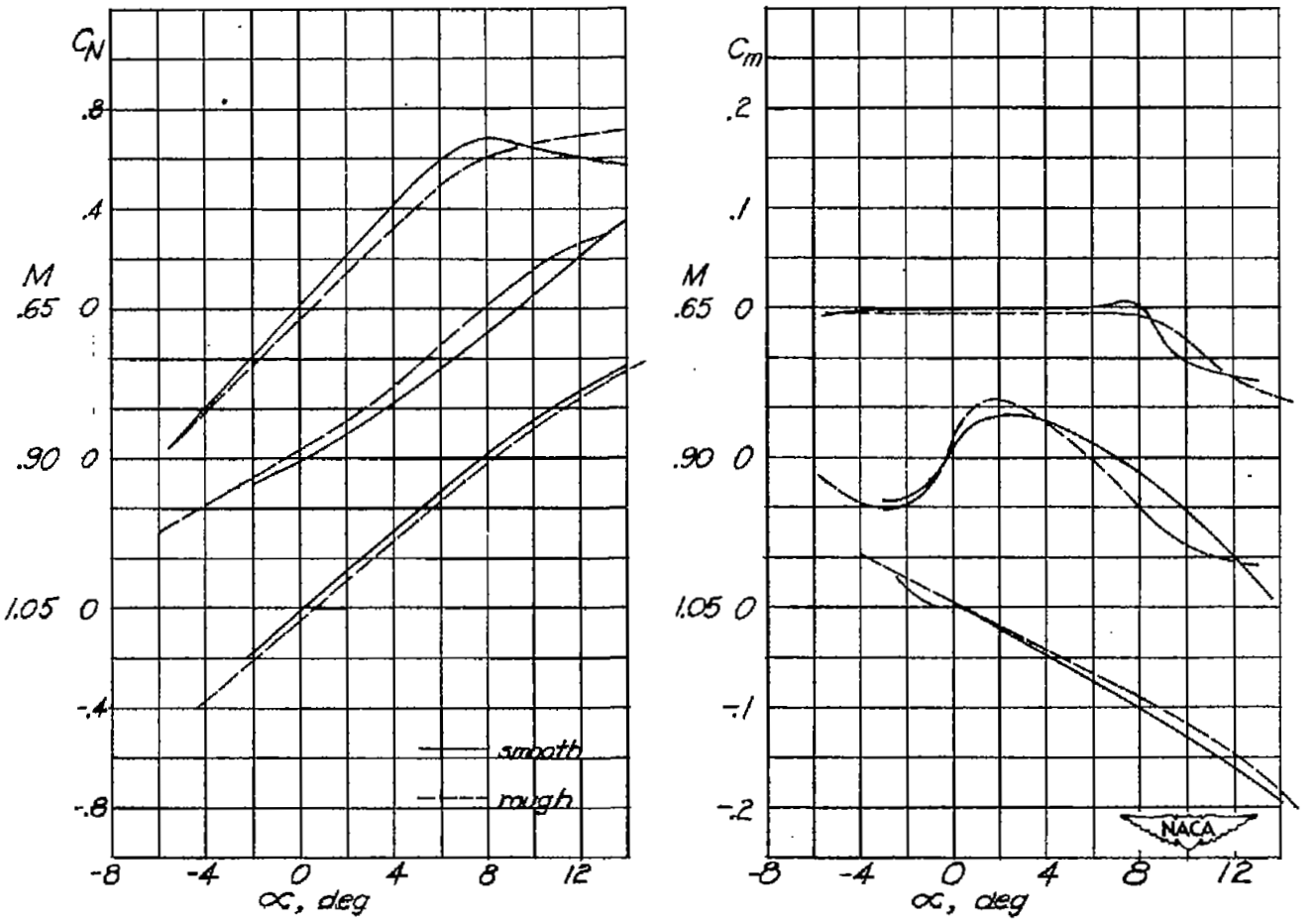

(a) Variation of lift and pitching-moment characteristics with angle of attack.

Figure 16.- Effect of leading-edge roughness on the force and moment characteristics of the NACA 65-010 airfoil at a Reynolds number of 0.7×10^6.

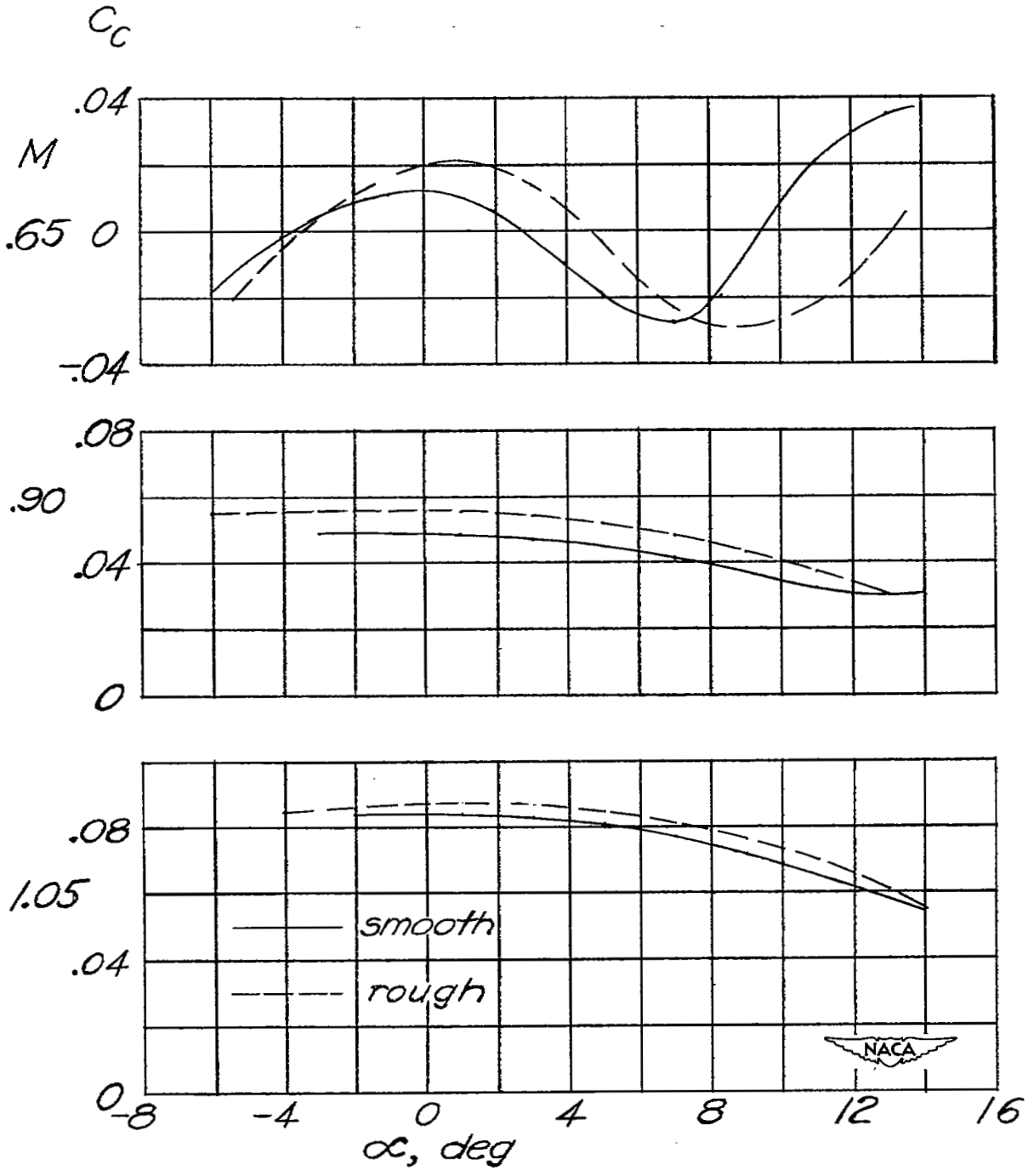

(b) Variation of chord-force coefficient with angle of attack.

Figure 16.- Concluded.

[redacted]

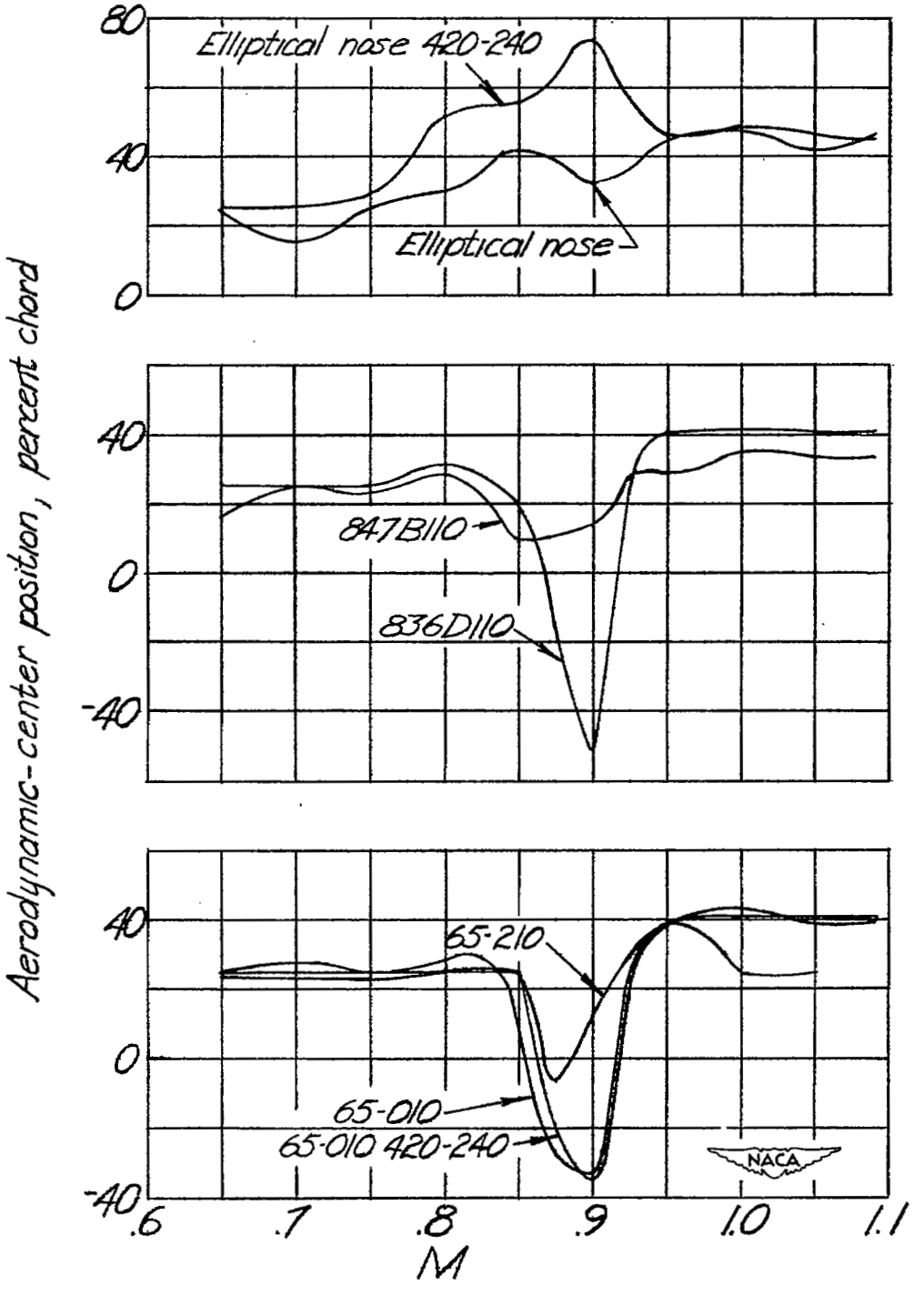

(a) $\alpha = 0^\circ$.

Figure 17.- Variation of the aerodynamic-center position with Mach number at two different angles of attack for the seven test airfoils.

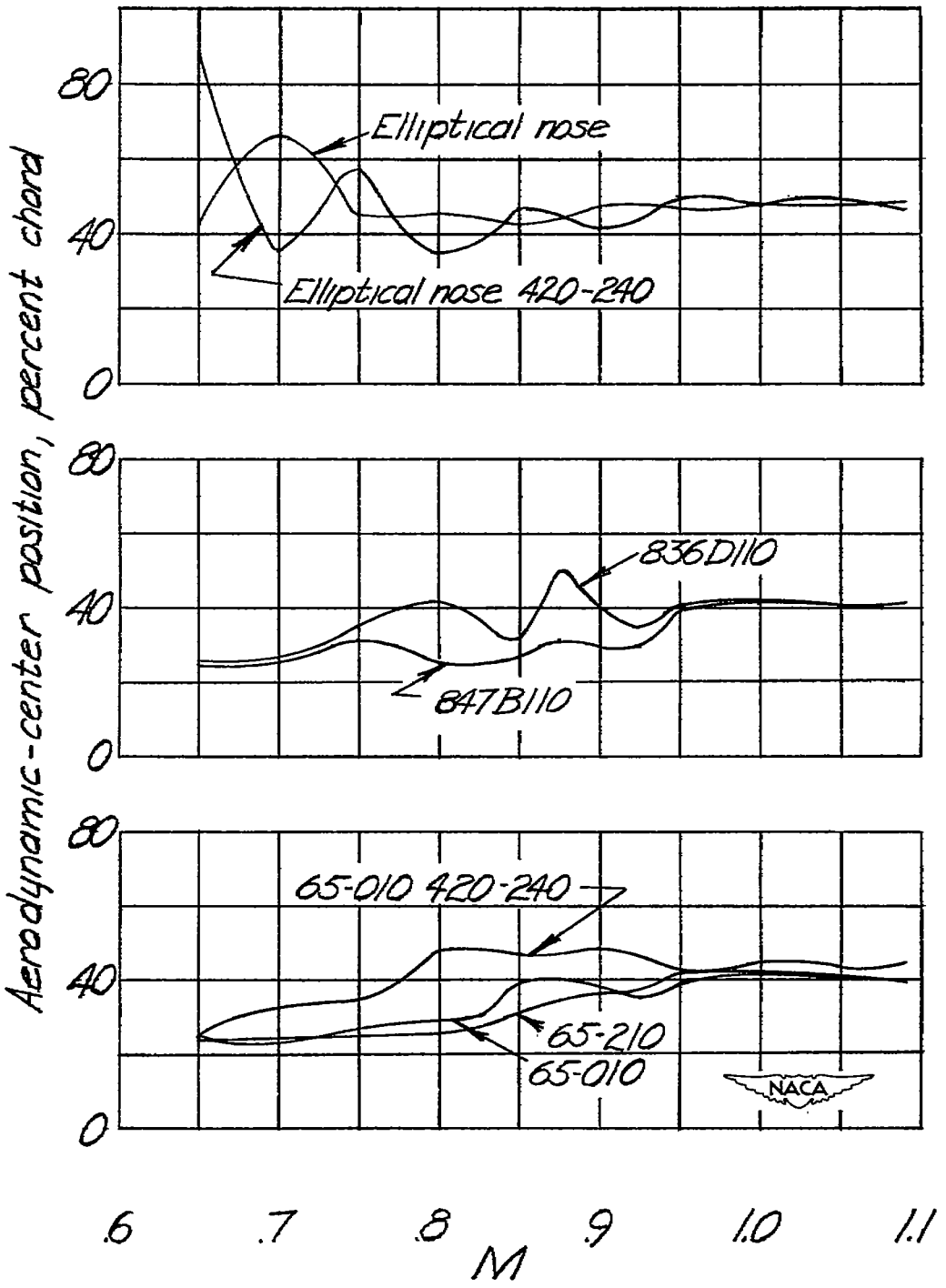

(b) $\alpha = 4^{\circ}$.

Figure 17.- Concluded.

[redacted]

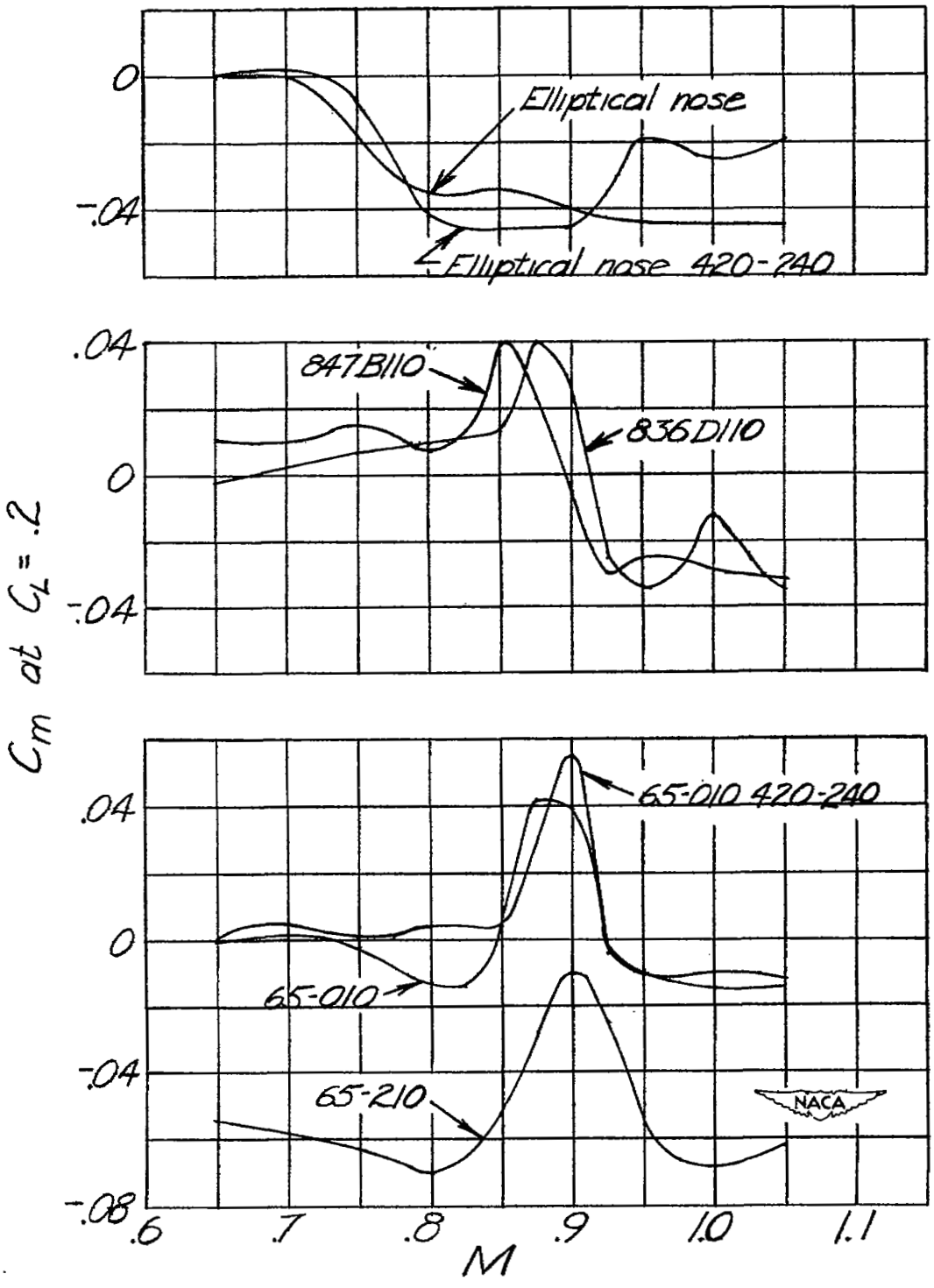

Figure 18.- Variation of the pitching-moment coefficient with Mach number at a lift coefficient of 0.2 for the seven test airfoils.

[redacted]

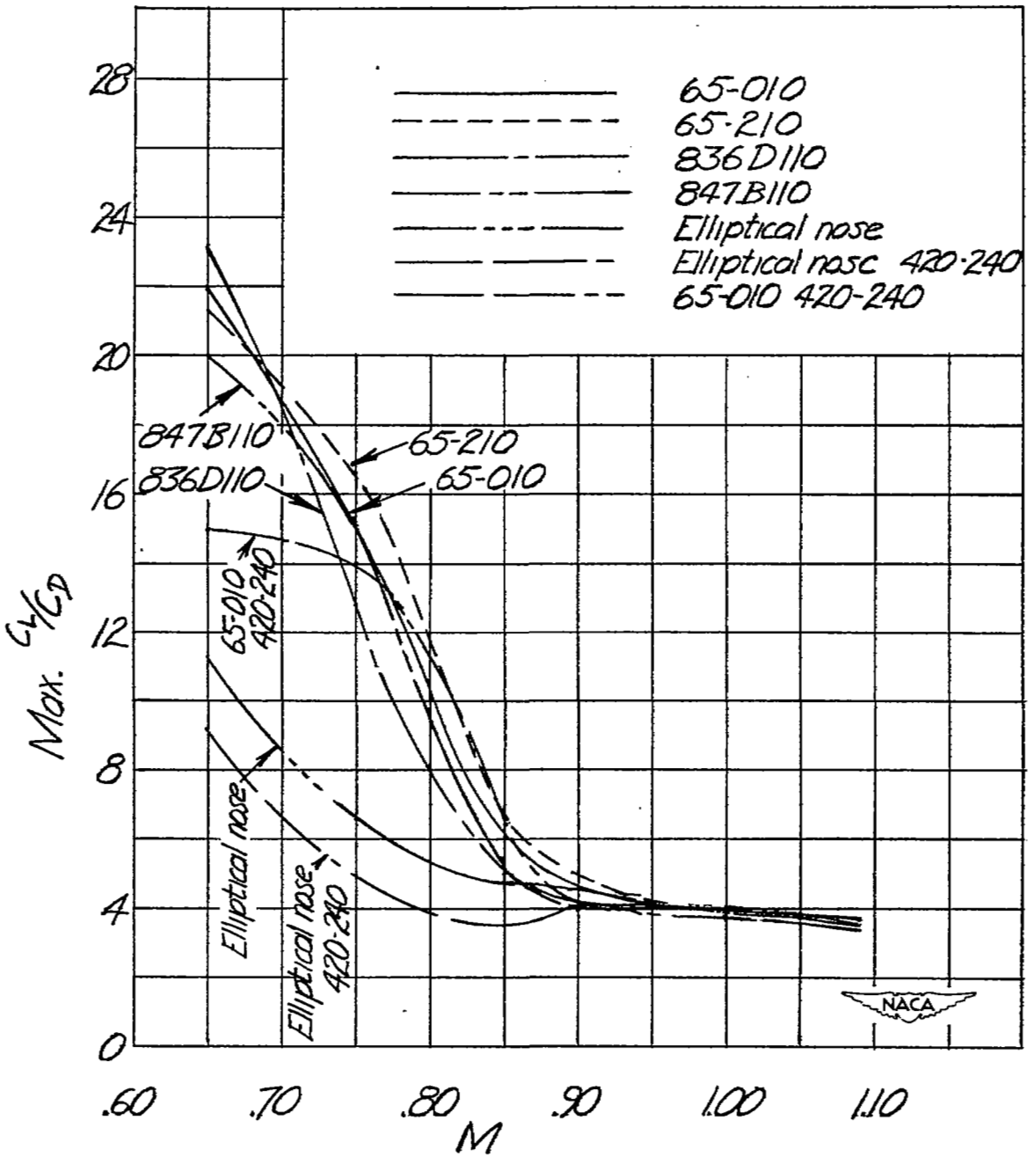

Figure 19.- Variation of maximum value of lift-to-drag ratio with Mach number for the seven test airfoils.

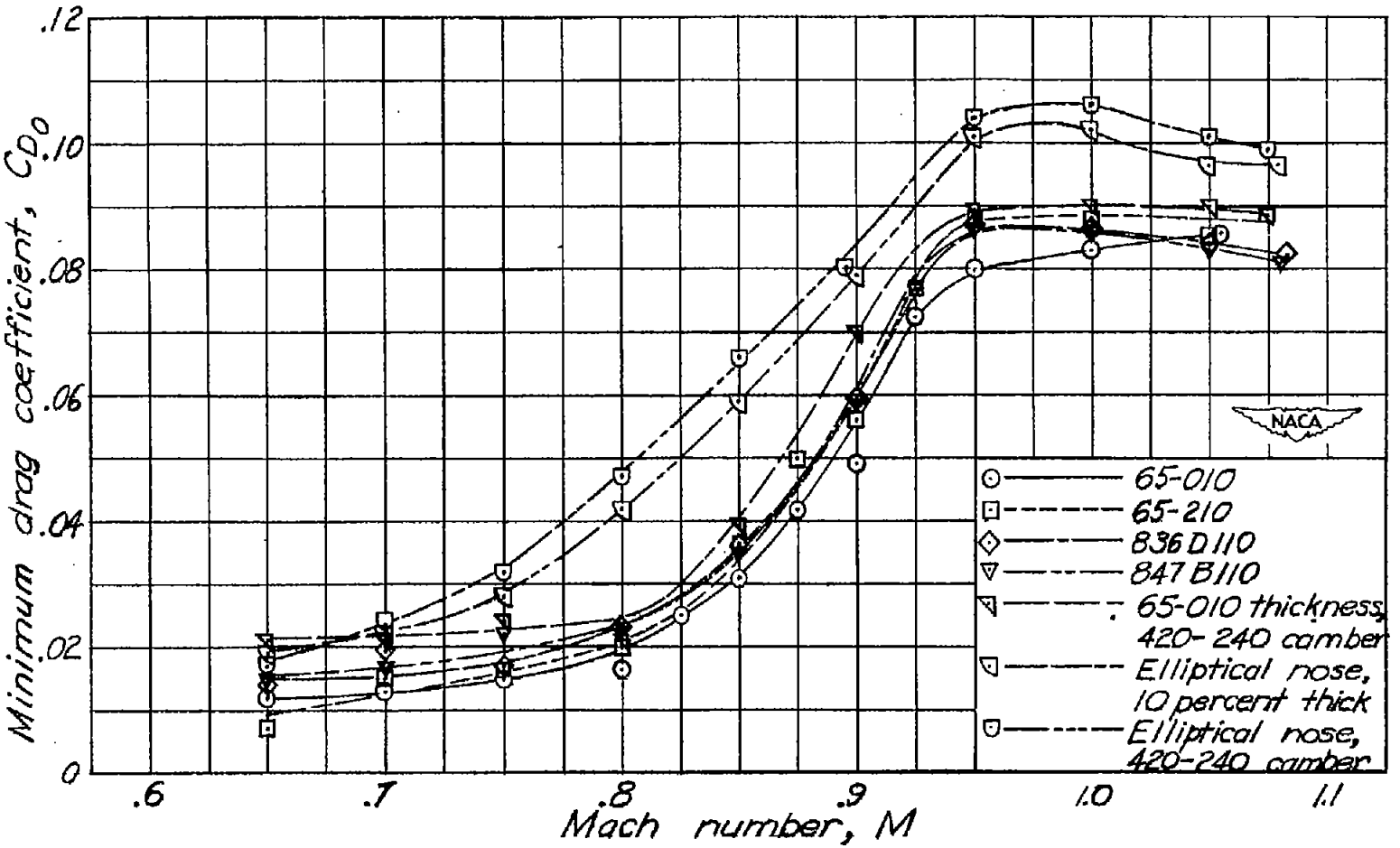

Figure 20.- Variation of minimum drag coefficient with Mach number.